10. DC Machines

10.1 Principles of Operation of DC Machines

a) The Main Magnetic Field:

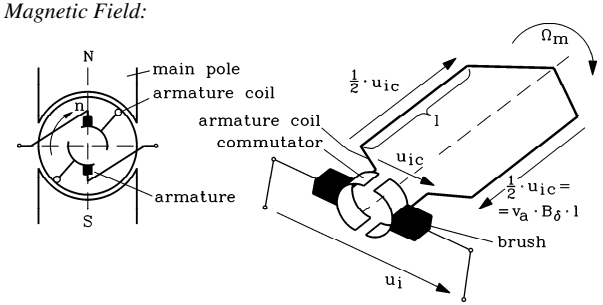

a) b)

Fig. 10.1: Principle of operation of DC machines:
a) Axial cross section of a two-pole machine with a single rotor coil,
b) Due to motion induction, an ac-voltage is induced in the moving rotor coil. The ac-voltage is rectified by the fixed "brushes" that are sliding on the commutator.

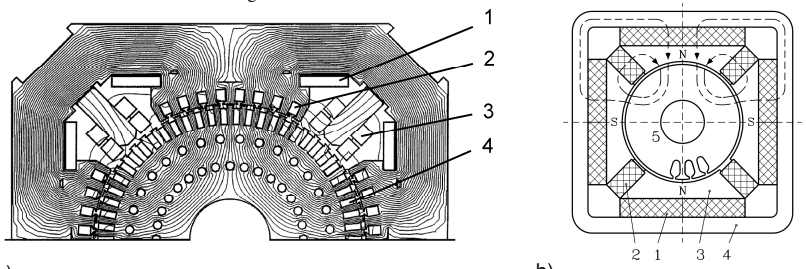

a) b)

Fig. 10.2: Four-pole dc machines: a) electric field excitation: calculated *B*-field at rated load (axial cross section of the upper half of the machine), field winding 1, compensating winding 2, commutating winding 3, armature winding 4,
b) permanent magnet field excitation: The flux density in the air gap is increased by flux concentration, no commutation poles, no compensating winding: 1, 2: magnets, 3: pole shoe, 4: yoke, 5: rotor

Fig. 10.1a shows a sketch of the axial cross section of a simple two-pole dc machine. The stator consists of a magnetic north and south pole. The field of the poles is excited by permanent magnets or an electric dc-excitation via field coils (Fig. 10.2). The magnetic flux per pole causes a magnetic field in the air gap field $B_\delta(x)$. $B_\delta(x)$ is schematically shown in Fig. 10.3, together with the linear unrolled stator poles that are electrically excited via field coils with the **field current (exciting current)** I_f. Likewise, the closing of the magnetic field lines in the stator via the stator yoke, the air gap and the rotor are shown. This **main field** is perpendicular to the air gap, becomes zero and changes polarity in the pole gaps (**"neutral zone"**). It is almost constant $B_{\delta,m}$ under the pole shoes, because the air gap is constant.

If a closed field line of the main field of Fig. 10.3 is used as curve *C* for application of *AMPERES*'s law to calculate the air gap field ($N_{f,pole}$: number of turns per field coil per pole),

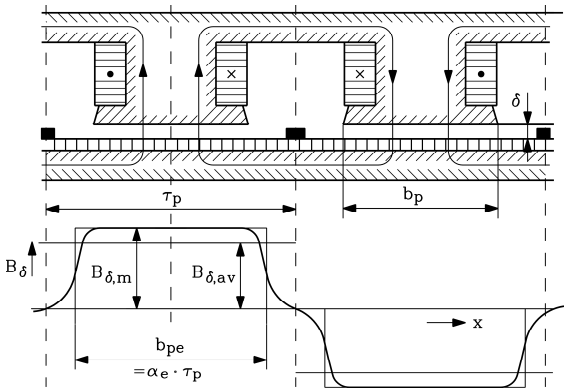

Fig. 10.3: Main magnetic field of an electrically excited dc machine: above: field lines, below: normal component of the air gap field. The influence of the rotor slot openings is not considered.

$$\oint_C \vec{H}\cdot d\vec{s} = \Theta \quad \Rightarrow \quad 2(H_{Fe}\Delta_{Fe} + H_\delta \delta) = 2(V_{Fe} + V_\delta) = 2N_{f,pole}I_f = 2V_f \tag{10.1}$$

the air gap field is given by (10.2).

$$B_{\delta,m} = \mu_0 H_\delta = \mu_0 \frac{N_{f,pole}I_f - H_{Fe}\Delta_{Fe}}{\delta} \tag{10.2}$$

As long as the iron is not saturated, it is $H_{Fe} \approx 0$ ($V_f = V_\delta$), and $B_{\delta,m}$ increases linearly with the field current. The influence of rotor slots on the air gap field is neglected in Fig. 10.3. In reality, the magnetic flux fringes in the rotor teeth due to the slotting (Fig. 10.2a), where the magnetic field is about two times as high as in the neighbouring air gap. Above 1.8 T **tooth flux density**, the iron saturates significantly, and the demand for magnetising current of the iron becomes noticeable beside the demand of the air gap, as the field current I_f increases ($V_f = V_\delta + V_{Fe}$).

Result:
The increase of the air gap field above 0.8 ... 0.9 T with increasing field current is less than linear, because of the saturation of the iron.

b) Voltage Induction:
The simplified rotor of Fig. 10.1a consists of an iron cylinder built from laminated iron with diameter d_r, length l and two slots that contain the rotor coil, the number of turns per coil is assumed to be $N_c = 1$. The rotor iron stack is fixed to the shaft. A copper segment is soldered to each of the two coil ends. Two fixed carbon pieces (**"brushes"**) are connected to the terminals and are sliding on the copper segments as the rotor rotates. Mica is used between two copper segments to insulate them. This assembly of copper segments and mica insulation in between is called **commutator**. If the rotor rotates with speed n, the coil sides travel with the circumferential speed (10.3) along the air gap field.

$$v_a = d_r \pi n = 2 p \tau_p n \tag{10.3}$$

In each coil side, an electric field strength $\vec{E}_b$ is induced via **motion induction**. The machine is designed to obtain a **maximum** value of $\vec{E}_b$: The conductors and the field are oriented perpendicularly. In the air gap, the field is almost perpendicular to the circumferential coordinate x, because of the small air gap width δ and the high ratio of permeability μ_{Fe}/μ_0 (Fig. 10.2). Outside of the rotor in the winding overhang the magnetic field is negligible small. The induced voltage per coil side is given by the integral of the electric field $\vec{E}_b$ along the coil side. The sum of voltages of both coil sides gives the alternating coil voltage $u_{i,c}(t)$ that is measurable at the terminals of the commutator.

$$u_{i,c}(t) = 2\int_l \vec{E}_b \cdot d\vec{s} = 2\int_l (\vec{v}_a \times \vec{B}_\delta) \cdot d\vec{s} = 2 v_a B_\delta l \tag{10.4}$$

The left brush in Fig. 10.1b **always** touches the sliding element of the commutator that is connected to the coil side under the left pole, the right brush the one connected to the side of the coil under the right pole. Therefore, the polarity of the induced voltage – as seen from the brushes – remains constant, because it is always positive under the left pole (e.g. N-pole) (**"plus-brush", A-brush**), and negative under the right pole (S-pole) (**"minus-brush", B-brush**). Hence, the induced voltage picked up by the brushes is given by the sum of the induced voltages of the two coil sides. It is a **dc voltage**, which is a rectification of the **ac voltage** within the moving coil. The coil sides are alternately under the N- and the S-pole. Hence, the polarity of the coil voltage alternates with the rotating speed of the rotor n. If the machine has $2p$-poles (e.g. $2p = 4$), the number of polarity changes per revolution increases with p and the frequency of the ac voltage increases by the same factor, called **armature frequency**.

$$f_a = n \cdot p \tag{10.5}$$

If the rotor coil has N_c turns, the induced voltage is N_c-times as large.

The course with time of the induced ac voltage is determined by the spatial distribution of the air gap field along the circumferential coordinate x because of $x = v_a t$ (Fig. 10.4). The corresponding amplitude of the voltage is determined by the maximum value of the air gap field $B_{\delta m}$.

$$u_{i,c}(t) = 2N_c v_a l B_\delta(x) = 2N_c v_a l B_\delta(v_a t) \tag{10.6}$$

$$\hat{U}_{i,c} = 2N_c v_a l B_{\delta,m} \tag{10.7}$$

c) Generation of Almost Ideal DC Voltage:
The rectified voltage (Fig. 10.4) is not ideally constant. Therefore, dc machines are built with a higher number of armature coils (rotor coils) that are connected in series. The coil sides are arranged in neighbouring slots. The distance between the slots (**slot pitch**) is determined by the number of rotor slots Q_r.

$$\tau_r = d_r \pi / Q_r \tag{10.8}$$

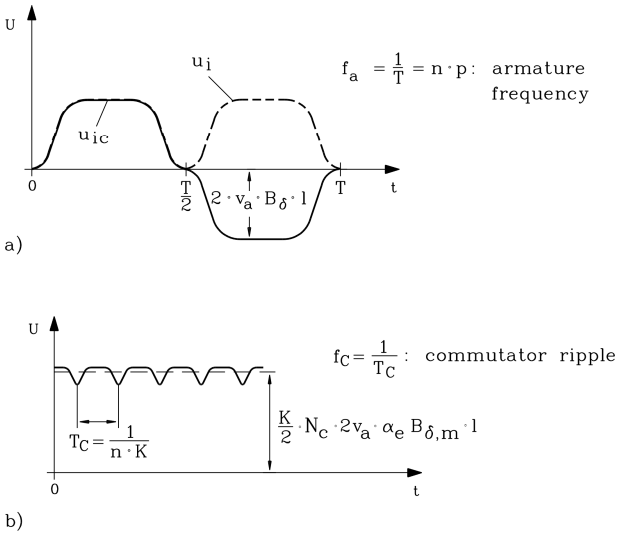

Fig. 10.4: a) AC coil voltage $u_{i,c}(t)$ and rectified voltage $u_i(t)$ of an armature coil
b) Rectified voltage between plus and minus brush at $K/2 = 4$

In neighbouring coils, the ac voltage is induced with phase shift τ_r/v_a. Hence, in the sum of the voltages of the individual coils the "voltage sag" due to the small field in the neutral zone becomes equalised. The more armature coils are used, the smoother the rectified voltage is (Fig. 10.4b). As the beginning and the end of each coil is connected to a commutator copper segment, more commutator segments are needed in this case. The series connection of coils is obtained by soldering the end of one and the beginning of the next coil together to a commutator segment. Therefore, two-pole machines with a commutator with K segments contain $K/2$ coils between plus and minus brush.

Example 10.1-1:
If the number of coils is 30, the remaining ripple of the voltage measured between two brushes values less than 2 % of the average value of the voltage.

Result:
In the series connected armature coils, placed in adjacent slots, voltage induction in each coil is time shifted. Due to the high number of coils, an almost ideal dc voltage is obtained via rectification by the commutator and brushes.

d) Calculation of the induced DC Voltage (back e.m.f.):
The average value of the rectified armature voltage can simply be determined by the spatial average value of the air gap field $B_{\delta av}$ according to Fig. 10.3, with τ_p being the **pole pitch**. The corresponding pole section with the air gap field at constant maximum value $B_{\delta,m}$ and the same air gap flux Φ as the real air gap field along the whole pole pitch is called **"equivalent pole pitch"** b_{pe} (from now on $B_{\delta,m}$ is denoted as B_δ).

$$B_{\delta,av} = \frac{1}{\tau_p}\int_0^{\tau_p} B_\delta(x)dx = \alpha_e B_{\delta,m} \tag{10.9}$$

$$\Phi = b_{pe} l B_\delta = \alpha_e \tau_p l B_\delta \tag{10.10}$$

The equivalent pole pitch is by the **equivalent pole arc ratio** α_e (= ca. 0.7) smaller than the real pole pitch: $b_{pe} = \alpha_e \tau_p$. Therefore, the average value of the rectified armature voltage is:

$$u_{i,av} = 2N_c v_a l \alpha_e B_\delta \tag{10.11}$$

In the case of a two-pole machine with K coils, it is:

$$u_{i,av} = U_i = (K/2)\cdot 2N_c v_a l \alpha_e B_\delta \quad . \tag{10.12}$$

The frequency of the remaining voltage ripple f_C is determined by the total number of coils, which is K, the number of the commutator segments, and the rotational speed:

$$f_C = n \cdot K \tag{10.13}$$

Using the circumferential speed of the rotor v_a and the total number of conductors of the rotor winding z (10.14), the **induced dc voltage** for a two-pole machine (p = 1) is obtained (10.15):

$$z = 2KN_c \tag{10.14}$$

$$U_i = (K/2)\cdot 2N_c v_a l \alpha_e B_\delta = (z/4N_c)\cdot 2N_c \cdot 2p\tau_p n \cdot l \alpha_e B_\delta = z \cdot n \cdot \alpha_e \tau_p l B_\delta = z \cdot n \cdot \Phi$$

$$\boxed{U_i = z \cdot n \cdot \Phi} \quad \text{(at } 2p = 2\text{)} \tag{10.15}$$

The formula for the induced voltage of a machine with a higher number of poles will be derived in Section 10.3.

Due to the saturation of the iron, the flux does not increase linearly with the field current. Therefore, the induced voltage **does not increase linearly** with the field current. Fig. 10.5 shows the **armature voltage** – measured between plus and minus brush – at no-load generator operation. No load means, that no current flows in the rotor winding. The rotor is driven by an external motor to get generator operation. Therefore, the no-load voltage U_{a0} at the brushes equals the induced voltage U_i which can be measured directly.

Result:
The induced voltage increases linearly with the speed and the flux, but not linearly with the field current.

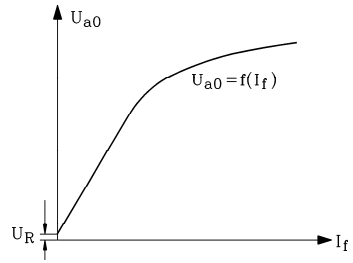

Fig. 10.5: **No-load characteristic** of a dc machine measured in generator operation: The induced voltage does not increase linearly with the field current due to the saturation of the iron.

e) Technology of Rotor Winding (Armature Winding), Commutator and Brushes:

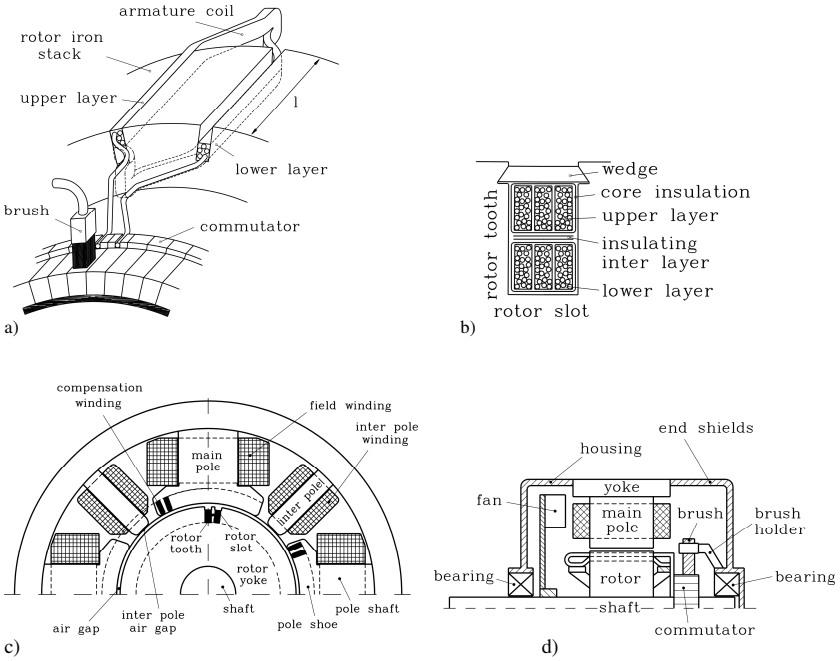

Fig. 10.6: Components of a dc machine:
a) rotor, rotor coil (here: from round-wire), commutator, brush
b) cross section of the rotor two layer winding from round wire, u = 3 coils per slot and layer, N_c turns per coil
c) axial cross section of a compensated, 4-pole dc machine
d) longitudinal cross section of a dc machine

At $K/2$ = 30 coils between plus and minus brush, K = 60 commutator segments are required. The width of the commutator segments in circumference direction is at least 2.9 mm, due to

mechanical limitations. Considering the thickness of mica insulation of at least 0.3 mm between two segments, the minimum value of the **commutator pitch** is $\tau_{c,min}$ = 3.2 mm.

Fig. 10.6a shows the rotor with a single representative rotor coil (armature coil), realised as two layer winding similar as in the case of polyphase windings, the commutator with its numerous segments and a carbon brush. Due to the conductor and coil insulation, the rotor slots can by far not be realised as small as the commutator segments. Therefore, the rotor has generally

- a larger diameter than the commutator,
- significantly less slots than the commutator has segments.

Therefore, several coil sides are put side by side in one slot (e.g. u = 3, Fig. 10.6b).

Example 10.1-2:
Two-pole machine, u = 4 coil sides per slot and layer, Q_r = 15 rotor slots:

- rotor slots per pole: 7.5
- number of commutator segments: $K = u \cdot Q_r = 4 \cdot 15 = 60$

$$K = u \cdot Q_r \tag{10.16}$$

In reality, the width in circumferential direction of the brush shown in Fig. 10.6a is larger than the width of one commutator segment and has a larger cross sectional area, thereby covering generally between 2 and 5 segments at the same time. The larger area A that the current passes is required to obtain a satisfactory low **brush current density**. The steady-state brush current density must not be larger than about 10...14 A/cm^2, if the graphite brushes shall not be damaged by overheating.

At the moment, when the coils are shorted by the brush in the area of the neutral zone, (Fig. 1.1) the induced voltage is zero, because the field is there zero. So, no voltage is short-circuited.

The current density in the copper conductors is – depending on the cooling method of the machine – significantly larger than in the brushes. Typical values are 4 ... 8 A/mm^2 at enclosed machines with surface ventilation. The *OHM*ic resistance of copper increases, but the *OHM*ic resistance of graphite decreases with increasing temperature. The main part of the electric resistance bet-ween a brush terminal and a commutator segment is given by the contact resistance between the sliding surface of the brush and the surface of the commutator (**"contact resistance"**). The current passage occurs at individual contact points from the graphite to the copper. The number of contact points increases with increasing current density. Therefore, the voltage drop at the brush is almost independent of the brush current density J_b. It is about 1...1.5 V per brush. Hence, a voltage drop U_b of 2...3 V occurs between plus and minus brush (Fig. 10.7b).

10.2 Rotor Windings (Armature Windings)

10.2.1 Lap Winding

a) Basic Element of a Lap Winding:
The increase of the number of coils, starting from one armature coil between two brushes, to obtain a smaller ripple of the dc voltage (Section 10.1), is shown in Fig. 10.8. At each commutator segment, the end of one coil and the beginning of the next are connected. The

width (span) of the coils is the distance between upper and lower layer of the coil. It should be about one pole pitch, so that both coil sides are at about the same time exposed to maximum field in the air gap or respectively in the neutral zone. If the **commutator segment pitch** $\tau_C = d_{si}\pi/K$ is considered as "one" step, the coil pitch may be expressed in numbers of commutator pitches as **"coil pitch"** y_1. Hence, a coil pitch corresponding to one pole pitch comprises $K/(2p)$ commutator pitches. With the **front span** y_2 (Fig. 10.8) , the overall step at the commutator is 1.

$$y = y_1 - y_2 \tag{10.17}$$

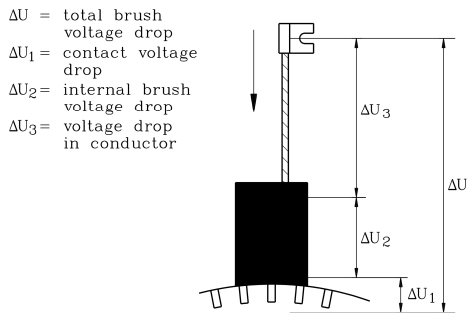

a)

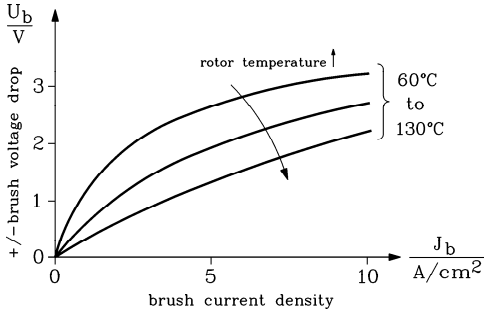

b)

Fig. 10.7: Brush contact:
a) The brush contact resistance is located mainly in the sliding zone of the brush: ΔU_1 is about 80% of ΔU.
b) At dc, the voltage drop U_b depends nonlinearly from the brush current density J_b and decreases with rising temperature.

Example 10.2.1-1:
K = 232, $2p$ = 4, $K/(2p)$ = 58, y_1 = 58, y_2 = 57, y = 1

b) Lap Windings with Two and More Poles:
Fig. 10.9 shows the series connected armature coils, until the whole pole pitch is covered by coils. If the winding is designed as a two pole winding, the upper layer winding on the left and the lower layer winding on the right share the same slots. The winding forms **an endless**

series connection of coils, that are electrically connected to the terminals at the commutator contact points via the brushes.

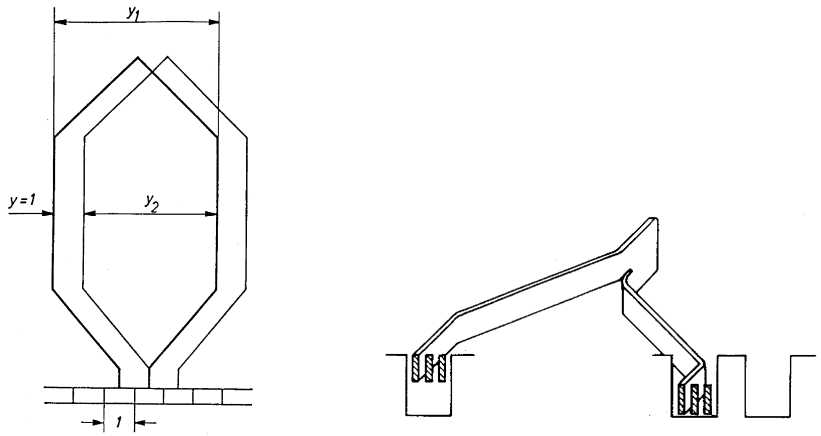

a) b)

Fig. 10.8: Formation of a lap winding:
a) Series connection of two coils at the commutator (unrolled depiction of the rotor),
b) Axial cut through the rotor with indicated slotting (here $u = 3$)

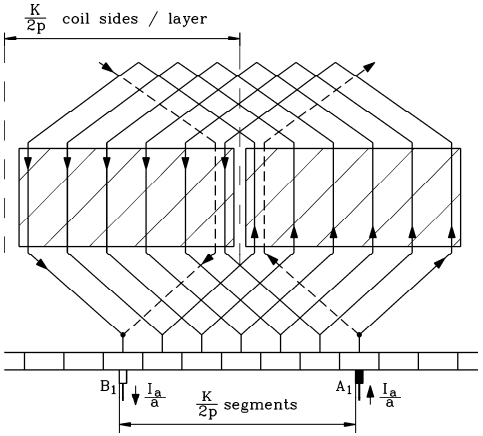

Fig. 10.9: Lap winding of one pole pair, unrolled depiction (hatched area: area of one pole shoe), $K/(2p) = 6$. The left coil sides belong to the upper layer, the right ones to the lower layer. For each slot, always two coil sides of different coils are arranged above each other.

In the case of a machine with 4, 6 or 8 poles, the winding continues to the left and to the right correspondingly, until the required number of poles is obtained. This is indicated in Fig. 10.10, where the $K/(2p)$ coils between two neighbouring brushes are replaced by an

equivalent loop (dashed line). Thereby, because of the alternating north- and south poles in the stator, a series of plus and minus brushes is obtained.

Example 10.2.1-2:
- If 440 V are induced between two brushes in Fig. 10.10, the plus brush A_1 is at +220 V, the minus brush B_1 at – 220 V.
- In the case of an extension to 6 poles, brush A_2 is again at +220 V, brush B_2 at –220 V, brush A_3 at +220 V and brush B_3 again at – 220 V.

Result:
All positive and negative brushes have the same electrical potential and can therefore be ***electrically connected in parallel****.*

c) Parallel Winding Branches of Lap Windings:
If the winding is supplied with dc current, the current I_b per brush splits according to Fig 10.9 in two equal parts, because it flows from the commutator segment to the left to the upper layer on one side, and to the right to the lower layer to the other coils. Both partial currents flow as coil currents I_c via these two winding branches to the minus brush, where they become one brush current again. Therefore, in the case of a machine with two poles, always **two parallel** winding branches exist. In addition, in the case of a machine with $2p$ poles, the p plus and the p minus brushes are connected in parallel themselves (Fig. 10.10). The total current as supplied from the outside to the armature I_a divides into $2p$ partial coil currents.

Result:
A lap winding has 2a parallel branches, and it is a = p. Each brush carries the brush current $I_b = I_a/a$. Note, that the minimum number of parallel winding branches is not "one" (a = 1), but "two" (2a = 2). Therefore, the symbol "a" signifies only "HALF of the number of parallel winding branches" in the case of dc machines, but "FULL number of parallel winding branches" in the case of three phase windings.

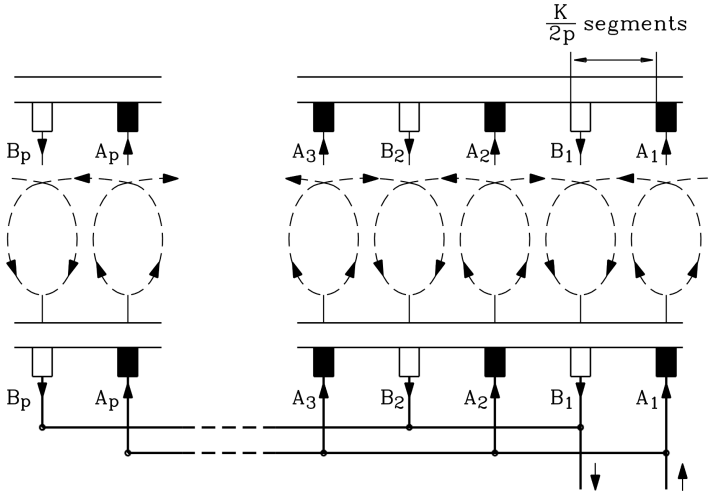

Fig. 10.10: Synthesis of a machine with 6 poles from a 2 pole machine (generally, $2p$ poles) by identical continuation of the lap winding, of the stator poles and of the brush arrangement.

Example 10.2.1-3:
Simplex lap winding, parameters: $Q_r = 26$, $2p = 4$, $u = 1$, $N_c = 1$.
- $a = p = 2$, $K = 26$, $y_1 = 6$, $y_2 = 5$, $y = 1$
- full winding pattern: Fig. 10.11.

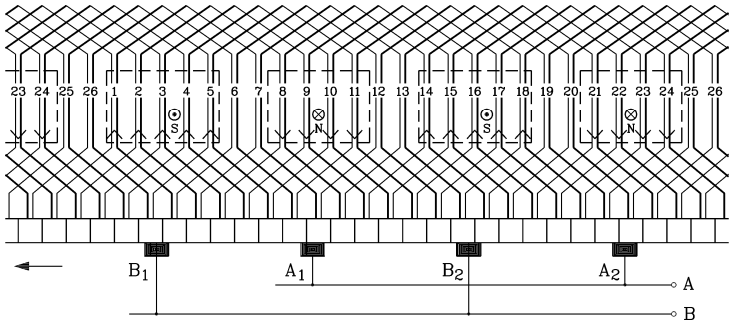

a)

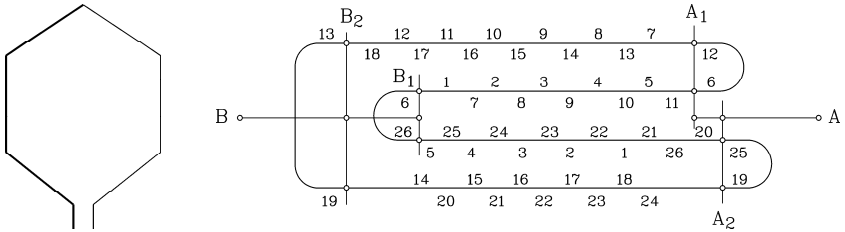

b) c)

Fig. 10.11: Lap winding: $Q_r = 26$, $2p = 4$, $u = 1$, $N_c = 1$, $a = p = 2$, $K = 26$, $y_1 = 6$, $y_2 = 5$, $y = 1$
a) Winding diagram (upper layer = left coil sides, lower layer = right coil sides)
b) Winding element = one armature coil (left: upper coil side, right: lower coil side)
c) Electrically effective connection of coil sides for the position of the brushes shown in a) (number above/below line: upper/lower coil side of two layer winding)

An increase of the number of poles does generally NOT increase the armature voltage U_a, but, because of the parallel winding branches, the armature current I_a is increased, so that the power $P = U_a I_a$ increases. Therefore, lap windings are suitable for machines with a high number of poles and large power.

d) Potential Equaliser of First Kind:
In reality, no machine can be built to obtain exactly the same voltage at the positive and negative brushes. Small potential differences between e.g. brush A_1 and A_2 in Fig. 10.11 can already significantly disturb symmetrical current distribution on the parallel brushes.

Example 10.2.1-4:
Machine with four poles (Fig. 10.11): Electrical potential between A_1 and $B_1 = B_2$ is 120% of rated voltage, whereas between A_2 and $B_1 = B_2$ it is only 80%. This leads to unsymmetrical current distribution: brush A_1: 120%, brush A_2 80 % of the rated brush current. Therefore,

brush A_1 is at electrical overload and wears out fast, resulting in too frequent necessary brush change.

To avoid unequal brush currents, **potential equalisers of 1st kind** are used. They are copper conductors in the rotor that connect commutator segments with (theoretical) equal electrical potential (Fig. 10.12). Hence, the equaliser pitch is:

$$y_V = K / p \qquad (10.18)$$

These equalisers carry the equalising current, which in the previous example is 20 % of the rated brush current, thus relieving the sensitive brush contact from over-current. Due to reasons of economy, generally only one equaliser per slot is used.

Example 10.2.1-5:
Simple example with very small slot number (Fig. 10.12):
- winding parameters: $2p = 4$, $2a = 4$, $u = 2$, $Q_r = 12$
- $K = 12 \cdot 2 = 24$, $y_1 = 6$, $y_2 = 5$, $y = 1$, $y_V = K/p = 24/2 = 12$
- e.g., segments 1 and 13 are connected, as they should always have the same electrical potential
- For the whole machine, 6 equalisers are needed to get one equaliser per slot.

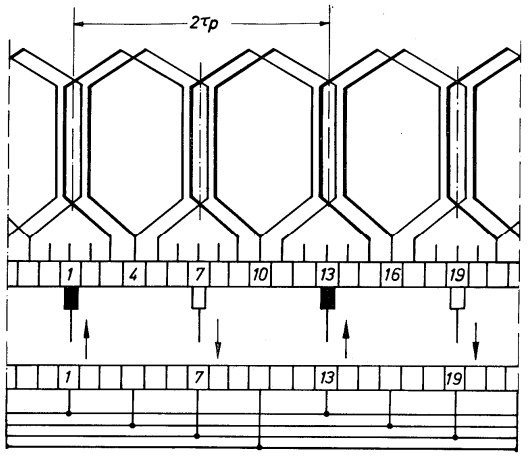

Fig. 10.12: Potential equaliser of 1st kind (simple example with very low slot number for educational purpose): $2p = 4$, $2a = 4$, $u = 2$, $Q_r = 12$, $K = 12 \cdot 2 = 24$, $y_1 = 6$, $y_2 = 5$, $y = 1$, $y_V = K/p = 24/2 = 12$ (e.g. segments 1 and 13 are connected).

e) Duplex Lap Winding, Potential Equaliser of 2nd Kind:
If each second commutator segment is not used for the lap winding, a second, identical lap winding can be added, which is connected to these segments. The mechanical equivalent is a double-threaded screw. Both windings – that are independent from each other – can be connected electrically in parallel by the brushes and are called **duplex lap winding**. Therefore, **4*p* instead of 2*p* parallel winding branches** are obtained. Thereby, at the same voltage and bar current density, the **power is doubled**. However, due to the imperfections of

real machines, both windings are not exactly identical, so again, **potential equalisers of 2nd kind, (*PUNGA*-equalisers)** are needed to keep equalising currents away from the brushes. Therefore, **duplex lap windings** are rarely used nowadays.

10.2.2 Wave Windings

a) Basic Element of a Wave Winding:
The series connection of neighbouring coils can also be performed alternatively to the lap winding in a second way (Fig. 10.13a): The end connections of one coil to the commutator segments are done at **almost** two pole pitches distance between beginning and end of a coil. Emphasis is put on the word "almost", because if, e.g. in the case of a machine with two poles, beginning and end would be at exactly two pole pitches distance, both ends of a coil would be at the same commutator segment and therefore the coil would be shorted. Therefore, the winding pitch is generally chosen according to (10.19).

$$y = y_1 + y_2 \quad , \quad y \neq K/(p) \text{ , but } y_1 \approx K/(2p) \tag{10.19}$$

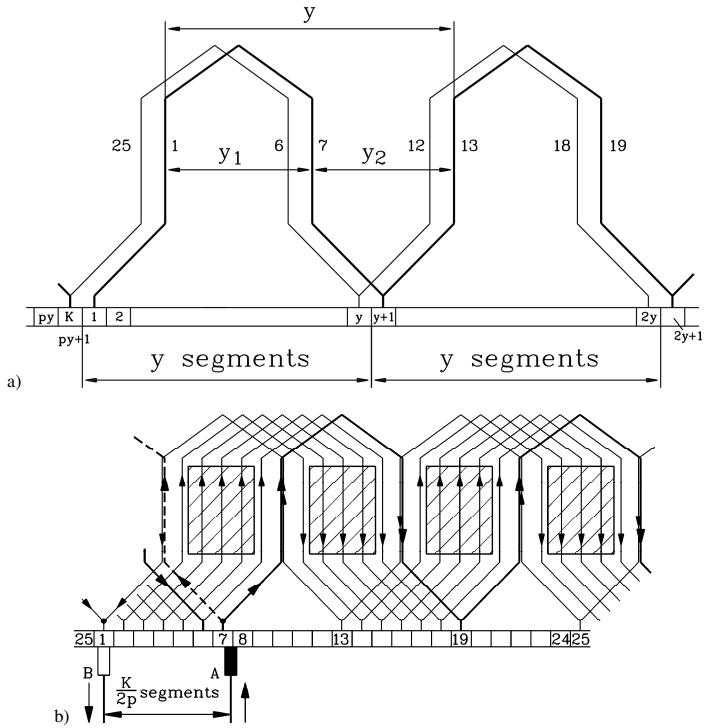

Fig. 10.13: Simplex wave winding (shaded area: pole shoes):
a) Generation of a wave winding from series connected armature coils, forming a "wave line" along the circumference of the armature. The first and second wave line, displaced towards each other by one segment pitch, are shown.
b) One armature branch of wave winding for four poles. The second armature branch starts at the coil indicated by the dashed line.

b) Wave Windings with Two and More Poles:
Fig. 10.13a is considered to determine the pitches y and y_2. The ends of the first coil are connected to segment 1 and to segment $y + 1$. The next coil is between segments $y + 1$ and $2y + 1$ etc., until, after connecting coils for all p pole pairs, the p^{th} coil reaches segment $py + 1$. This last segment is number K, which equals the total number of commutator segments. Hence, p series connected coils are between this segment and its neighbouring segment 1. Due to $K = py + 1$, it is derived for any wave winding:

$$y = \frac{K-1}{p} = \text{integer} \tag{10.20}$$

By that, the conditions $y \neq K/p$ and $y_1 \approx K/2p$ are satisfied.

c) Parallel Winding Branches at Wave Windings:

Example 10.2.2-1:
Wave winding with simplified data for a better understanding (Fig. 10.13b): $2a = 2$, $u = 1$, $Q_r = 25$, $2p = 4$,
- $K = 25$, $y = (K\text{-}1)/p = 12$, $y_1 = 6$, $y_2 = 6$
- Coil connection:
  1 (upper layer, UL) → 7 (lower layer, LL) → 13 (UL) → 19 (LL) → 25 (UL) → 6 (LL)...,
- In Fig. 10.13b, the "filling" of the armature slots by the series connected coils as wave lines is shown, beginning with segment 7 and ending with segment 1.
- If the wave lines continue from the right to the left, in the region of the 1st pole pitch, all upper layer positions in the slots are occupied, in the following pole pitch all lower layer positions, in the next pole pitch all upper layer positions etc., ending after $(K-1)/(2p) = 24/4 = 6$ wave lines. Half of all positions in the slots are occupied.
- The same procedure can be done – beginning at segment 7 – continuing from the left to the right, where now all vacant lower layer positions in the 1st pole pitch, in the next all vacant upper layer windings etc. are occupied (dashed line in Fig. 10.13b). Again, after 6 wave lines, all slot positions are occupied.
- Therefore, the winding system is **closed in itself**. Two parallel branches have been generated – e.g. starting from brush A in Fig. 10.13b – to the left into the next lower layer, and to the right into the next upper layer.

Result:
The simplex wave winding has always two parallel branches: a = 1, 2a = 2.

One plus and one minus brush are sufficient for the electrical connection to the terminals (Fig. 10.13), as only two parallel winding branches exist. However, the total current I_a equals the brush current I_b. To keep the brush current density below 12 A/cm^2, both brushes must have a large cross sectional area. Two big brushes for a dc machine are rarely used.

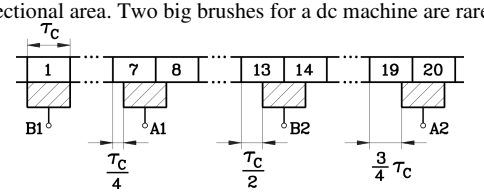

Fig. 10.14: Arrangement of the brushes along the commutator for the wave winding of Fig. 10.13 at fully applied set of brushes (here simplified: brush width = segment width)

Instead of two big brushes, 2*p* small brushes are used, distanced by one pole pitch, like in lap windings (Fig 10.14). In Fig. 10.13, the two coils connected to the A-brush, span from segments 7 and 8 to segments 19 and 20, respectively. At this time, the slot conductors of these coils lie in the neutral zone, where the air gap field is zero, so **no** voltage is induced. Therefore, a second A-brush can be applied at two pole pitches distance from the first A-brush and connected in parallel to the first. Then – as with the lap winding – only coils at zero voltage are shorted (7-19, 8-20), which are therefore at the same electric potential. So, these coils at zero voltage act as potential equalisers of 1st kind; we say, the wave winding is **self-equalising**. In the same way, a second B-brush at segments 13, 14 can be applied and connected in parallel to the first B-brush at segment 1. Thereby – as in the case of a lap winding – one brush per pole is obtained at the commutator (Fig. 10.14).

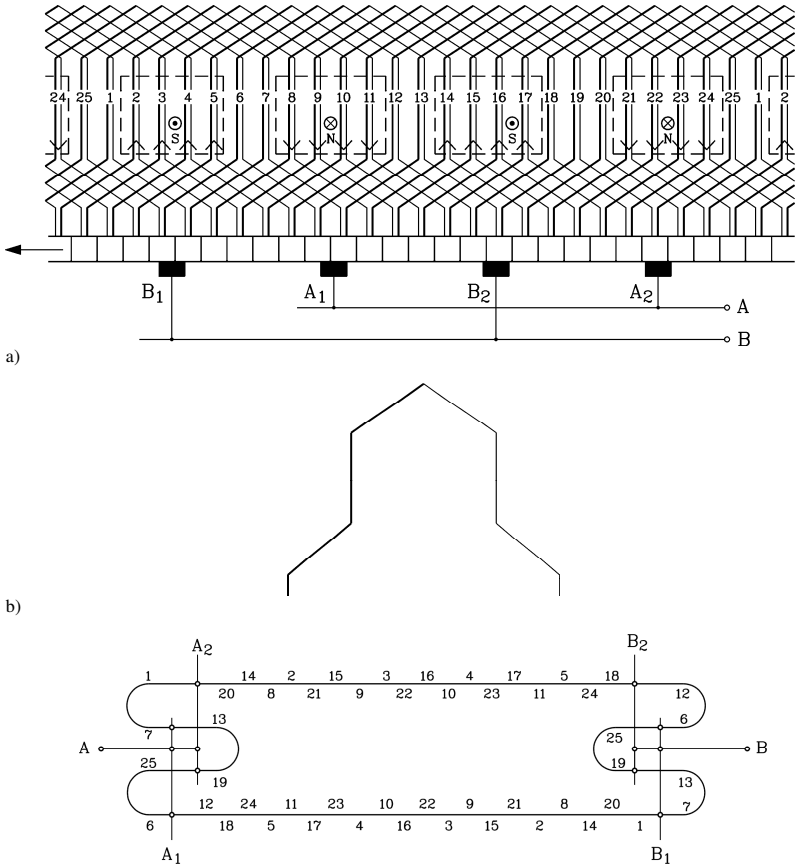

Fig. 10.15: Wave winding: $Q_r = 25$, $2p = 4$, $u = 1$, $N_c = 1$, $a = 1$, $K = 25$, $y_1 = 6$, $y_2 = 6$, $y = 12$
a) complete winding scheme (compare with Fig. 10.13)
b) winding element = one armature coil (left: upper coil side, right: lower coil side)
c) electrically effective connection for the position of the brushes relative to the commutator as shown in a) (number above/below line: upper/lower coil side)

d) Duplex Wave Winding:
Duplex wave windings, arranged as two wave windings similar to duplex lap windings, are rarely used due to the large equalising currents between the individual windings. Likewise, special windings like the combination of lap and wave winding (**"frog-leg"- or *LATOUR*-winding**) are rarely used.

10.2.3 Comparison between Lap and Wave Winding

Lap Winding	*Two-Circuit Winding*
number of parallel winding branches = number of poles $2a = 2p$	Number of parallel winding branches is always 2 $2a = 2$
first kind equaliser required	self equalising
high currents possible	current limited to about 500 A
high power possible (up to about 12 MW)	power limited (about 300 kW)

Table 10.1: Comparison between lap and wave winding

In the case of a wave winding, the power is limited, because only two parallel winding branches exist. Typical limits for current per branch are about 250 A, corresponding to an upper limit of 500 A total current per winding. Therefore, large power DC machines are only designed with lap winding, e.g. a 6 MW dc drive with 18 poles, hence 18 parallel circuits, in a steel mill.

10.2.4 Voltage Limit of a DC Machine

Caused by the mechanical brush wear, there is carbon dust inside the dc machine. Due to the higher electric field density at the commutator segment edges and the conducting carbon dust, the **break down field strength** between two commutator segments is much smaller than in dry air at an electrically homogenous field, where it is about 40 kV/cm. The "**average" segment voltage** is the voltage between two commutator segments averaged over all segments between plus and minus brush.

$$U_{s,av} = U_a / (K/2p) \qquad (10.21)$$

It must not exceed 18 ... 20 V. The maximum "**local**" commutator segment voltage should stay below 35 V, to avoid flashover between two commutator segments.

Example 10.2.4-1:
- At 0.3 mm mica thickness, an average segment voltage of 20 V corresponds to a field strength of $E = 20/0.03 = 0.7$ kV/cm. This is significantly smaller than 40 kV/cm !
- At $K/(2p) = 30$ segments between two brushes, the value of the permissible dc armature voltage is $U_a = 30 \cdot 20$ V = 600 V.

Result:
Generally, dc machines are only designed for low voltage ($U_a < 1000$ V).

10.3 Induced Voltage and Electromagnetic Torque

a) Induced Voltage:
The total number of slot conductors in a machine is called the total **number of conductors** *z* (10.14). If these conductors would not be arranged in slots, but evenly distributed as a "current loading" along the rotor circumference (Fig. 10.3), the circumferential length *dx*

would contain $\frac{z}{2p\tau_p}dx$ armature conductors. Per pole, all conductors are series connected. Hence the induced voltage is given by

$$U_i = \int dU_i = \int_0^{\tau_p} B_\delta(x)\cdot l\cdot v_a \cdot \frac{z}{2p\tau_p}\cdot dx = z\cdot n\cdot l\int_0^{\tau_p} B_\delta(x)\cdot dx = z\cdot n\cdot \Phi \qquad (10.22)$$

This result is in accordance with (10.15) and shows that the bundling of the armature conductors in the slots does not have any influence on the induced voltage.

- In the case of a lap winding, where the series rotor coils per pole are connected electrically in parallel to the coils of the next pole, the induced voltage per pole equals the total induced voltage of the machine.
- In the case of wave winding with only two parallel branches, the coils of p armature poles are series connected, and the total induced voltage of the machine is p-times larger than that of one pole.

Generally, the **induced voltage** (**back e.m.f.**) is:

$$\boxed{U_i = z\frac{p}{a}\cdot n\cdot\Phi = k_1\cdot n\cdot\Phi = k_2\cdot\Omega_m\cdot\Phi} \quad , \quad k_1 = z\frac{p}{a},\ k_2 = \frac{k_1}{2\pi} \qquad (10.23)$$

Lap winding: $\frac{p}{a}=1$, wave winding: $\frac{p}{a}=p$.

At steady-state operation, no other voltage induction than the rotationally induced voltage occurs in the armature winding, because the main flux is excited by dc current, hence, it is constant with time.

b) Electromagnetic Torque:

If the winding is supplied with the **armature current (dc current I_a)** via the brushes, this current is converted into **ac current with amplitude I_a** by the commutator. Between each plus and minus brush, the current flows from plus to minus. The conductors between two brushes lie each under one main pole. The spatial distribution of current flow below the pole is at rest (Fig. 10.16a). The current direction below the north and the south poles is opposite. As the armature coils are moved due to the rotation of the rotor, they alternately have to carry positive and negative current while passing alternately north and south poles (Fig. 10.17).

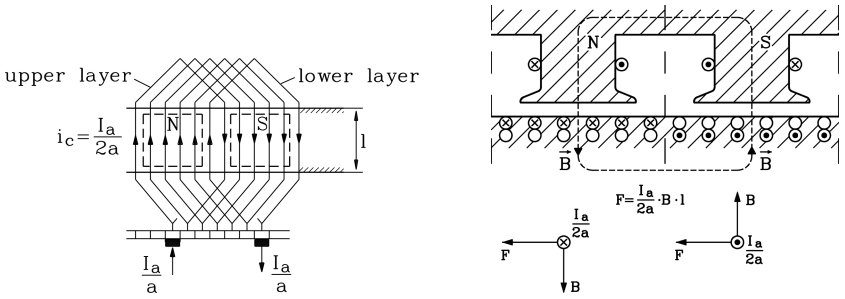

Fig. 10.16: Current flow in the armature winding: a) Only one direction of current flow exists per pole, b) Force generation by the stator magnetic field B on a current in an armature conductor.

Nevertheless, the spatial distribution of the rotor current relative to the main field is constant. Therefore, the torque generation is identical for all poles. The armature current divides into $2a$ parallel armature branches resulting in a coil current per slot of $I_c = I_a/(2a)$. Within a given segment dx, the contained ampere-turns are $\frac{I_a}{2a}\cdot\frac{z}{2p\tau_p}dx$. The electromagnetic *LORENTZ* force in the air gap on these ampere-turns are (Fig. 10.16b):

$$dF(x) = \frac{I_a}{2a}\cdot\frac{z}{2p\tau_p}dx\cdot l\cdot B_\delta(x) \qquad (10.24)$$

The generated torque per pole $M_{e,pole}$ is the sum of all forces $dF(x)$ of a pole segment F_{pole}, multiplied by the lever $d_r/2 = p\tau_p/\pi$. All $2p$ poles generate the same value of $M_{e,pole}$, so the total electromagnetic torque M_e is:

$$M_e = 2p\cdot M_{e,pole} = 2p\cdot\frac{p\tau_p}{\pi}\cdot F_{pole} = 2p\cdot\frac{p\tau_p}{\pi}\cdot\int_0^{\tau_p} dF \qquad \Rightarrow$$

$$M_e = 2p\cdot\frac{p\tau_p}{\pi}\int_0^{\tau_p}\frac{I_a}{2a}\cdot\frac{z}{2p\tau_p}\cdot l\cdot B_\delta(x)\cdot dx = \frac{1}{2\pi}\cdot z\frac{p}{a}\cdot I_a\cdot\Phi = k_2\cdot I_a\cdot\Phi$$

$$\boxed{M_e = k_2\cdot I_a\cdot\Phi} \qquad (10.25)$$

The torque can also be directly obtained from the **balance of power**. At motor operation and armature terminal voltage U_a, the total active power P_e supplied to the armature is in the consumer reference system (Fig. 10.18):

$$P_e = U_a I_a = (U_i + I_a R_a)I_a = U_i I_a + R_a I_a^2 \qquad (10.26)$$

The armature copper losses are considered by the total resistance of the armature winding R_a (**armature resistance**). The remaining power is the **internal power P_δ**. It is converted into mechanical power P_m by *LORENTZ* forces via the electromagnetic torque M_e.

$$P_\delta = U_i I_a = \Omega_m M_e = P_m \quad \Rightarrow \quad M_e = \frac{U_i I_a}{\Omega_m} = \frac{z\frac{p}{a}\cdot n\cdot\Phi}{2\pi\cdot n}I_a = \frac{1}{2\pi}\cdot z\frac{p}{a}\cdot I_a\cdot\Phi \qquad (10.27)$$

The result (10.27) is in accordance with the previously derived equation (10.25).

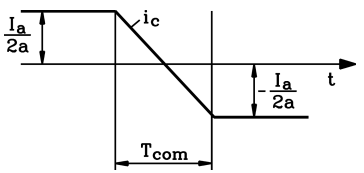

Fig. 10.17: The armature current per coil i_c is an alternating current.

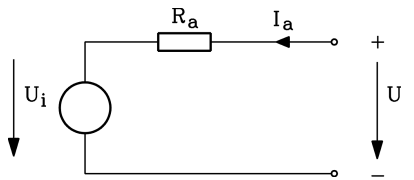

Fig. 10.18: Equivalent circuit of a dc armature winding in motor operation, feeding voltage U

Example 10.3-1:
200 kW dc machine at motor operation:
Rated armature voltage 430 V, n = 1470/min, d_r = 400 mm, $2p$ = 4, l = 190 mm, Q_r = 58 slots, u = 4, N_c = 1, α_e = 0.7, B_δ = 0.86 T, efficiency η = 92%

- Number of commutator segments $K = Q_r \cdot u = 58 \cdot 4 = \underline{232}$
- Total number of conductors $z = 2 \cdot K \cdot N_c = 2 \cdot 232 \cdot 1 = \underline{464}$
- Pole pitch $\tau_p = d_r\pi/4 = 400\ \pi/4 = \underline{314.2\ \text{mm}}$
- Main flux per pole $\Phi = \alpha_e \cdot \tau_p \cdot l \cdot B_\delta = 0.7 \cdot 0.3142 \cdot 0.19 \cdot 0.86 = \underline{35.9\ \text{mWb}}$
- Induced voltage $U_i = z \cdot (p/a) \cdot n \cdot \Phi = 464 \cdot (2/2) \cdot (1470/60) \cdot 0.0359 = \underline{408.5\ \text{V}}$
- Average voltage per segment $\dfrac{U_i}{K/(2p)} = \dfrac{408.5}{232/4} = \underline{7.04V} < 18...20\text{V}$
- Supplied electric power $P_e = P_{e,in} = P_{m,out}/\eta = 200/0.92 = \underline{217.4kW} = U_a I_a$
- Armature current $I_a = P_e/U_a = 217.4/0.43 = \underline{506A}$
- Internal power $P_\delta = U_i I_a = 408.5 \cdot 506 = \underline{206.7kW}$
- Electromagnetic torque $M_e = 206.7/(2\pi \cdot 1470/60) = \underline{1.343\ \text{kNm}}$
- Shaft torque at load:
  $M = P_{m,out}/\Omega_m = 200/(2\pi \cdot 1470/60) = \underline{1.299\ \text{kNm}}$

Balance of losses in the machine:

- Total losses: $P_d = P_{e,in} - P_{m,out} = 17.4$ kW converted into heat
- Thereof in the **armature**: $P_{d,a} = P_{e,in} - P_\delta =$ 217.4 - 206.7 = 10.7 kW
  - Thereof in the **brushes**: $P_b = U_b \cdot I_a =$ 2V · 506A = 1.0 kW
  - In the **armature resistance** (= *OHM*ic resistance of the armature and commutating winding (see Section 10.5)): $P_{Cu,a} = P_{d,a} - P_b = 10.7 - 1.0 = 9.7$ kW
- Mechanical braking loss torque of the rotor M_d = 1.343 -1.299 = 0.044 kNm, corresponding to the losses $P_{Fe} + P_R + P_z = 2\pi n M_d = P_\delta - P_{m,out} =$ 206.7-200 = 6.7 kW.
  - **Eddy current and hysteresis losses** P_{Fe} in the laminated iron core of the rotor,
  - **Additional losses** P_z: Eddy currents in the slot conductors due to current displacement, because ac current flows in the conductors
  - **Friction and windage losses** in the bearings, at the brushes and due to the cooling air flow.

10.4 Armature Reaction and Compensating Winding

a) Air Gap Field at No-Load (I_a = 0):
At **no-load** ($I_a = 0$), the requested m.m.f. for air gap and iron $V_f = V_\delta + V_{Fe}$ as a function of the circumferential coordinate x is constant along one pole pitch. It is given by the exciting ampere-turns $V_f = N_{f,Pole} I_f$ per pole. If the influence of the slot openings of the armature on the main pole air gap field is neglected, the corresponding B-field in the air gap

$$B_\delta(x) = \mu_0 \frac{V_f - V_{Fe}}{\delta(x)} \tag{10.28}$$

is also constant along the main poles and decreases in the pole gaps (Fig. 10.19a). In the **neutral zone** (q-axis), the field is zero and changes its polarity.

b) Air Gap Field at Load ($I_a > 0$):
When the armature winding carries current, the current carrying conductors excite an additional magnetic field, which is called **field of the armature reaction** (**armature quadrature-axis field**). The flux lines close via the rotor iron, the air gap and the stator iron (Fig. 10.19b). Due to reasons of symmetry, the centre of the corresponding field eddy is in the polar axis (d-axis). If this point is defined x = 0, the magnetising ampere-turns $V_a(x)$ increase linearly with x, because of the constant armature current loading (Fig. 10.19a below). The maximum value of $V_a(x)$ is reached at $x = \tau_p/2$, then, $V_a(x)$ decreases again linearly, because the armature current has opposite sign under the neighbouring pole.

$$V_a(x) = \int_0^x A(x)dx = A \cdot x \tag{10.29}$$

$$A = \frac{z \cdot \dfrac{I_a}{2a}}{2p\tau_p} \qquad \text{(armature current loading } A\text{)} \tag{10.30}$$

$$\Theta_a = V_a(x = \tau_p/2) = A\frac{\tau_p}{2} = \frac{z}{8ap} I_a = N_{a,Pol} I_a \qquad \text{(armature ampere-turns)} \tag{10.31}$$

In Fig. 10.19b, the **resulting field**, which is excited both from the exciting and the armature ampere-turns

$$B_\delta(x) = \mu_0 \frac{V_f + V_a(x) - V_{Fe}}{\delta(x)} \quad , \tag{10.32}$$

increases to the right and decreases to the left. As with increasing B_δ also the flux density in the rotor teeth increases, the iron saturates in the rotor teeth. Therefore, V_{Fe} is high in the right part of the pole, but it is almost zero in the left part, because of the decrease of the field when compared with zero-load. The increase of the air gap field in the right part of the pole is due to saturation SMALLER than the decrease in the left part. Hence, at load, the flux per pole Φ, which is proportional to the area below the field curve is <u>smaller</u> than at no-load.

$$\Phi = l \int_0^{\tau_p} B_\delta(x)dx = \Phi(I_a > 0) < \Phi(I_a = 0) \tag{10.33}$$

Result:
The additional saturation of the iron due to the armature quadrature-axis field (armature reaction field) causes a ***"flux loss"*** *$\Delta\Phi$.*

c) Influence of the Field Distortion on the Segment Voltage:
The armature reaction field causes the total air gap field to rise in the right and to decrease in the left half a pole (**field distortion**). Hence, in the parts of increased field, the induced coil voltage is larger than at zero-load, which may cause a too high voltage between two segments.

Example 10.4-1:
DC machine: Q_r = 34, u = 3, $2p$ = 4, lap winding, N_c = 2, $B_{\delta,m}$ = 0.9 T,

$\alpha_e = 0.7$, $n = 2000$/min, $d_{si} = 200$ mm, $l = 355$ mm

- Flux per pole: $\Phi = \alpha_e \tau_p l B_{\delta,m} = 0.7 \cdot 0.157 \cdot 0.355 \cdot 0.9 = 35.1\,\text{mWb}$, $K = Q_r \cdot u = 34 \cdot 3 = 102$
- Induced voltage: $U_i = z \cdot (p/a) \cdot n \cdot \Phi = 408 \cdot (2/2) \cdot (2000/60) \cdot 0.0351 = 477.4\,\text{V}$
- Rotor circumferential speed: $v_a = 2 p \tau_p n = 2 \cdot 2 \cdot 0.157 \cdot (2000/60) = 20.9\,\text{m/s}$
- Average voltage between two segments: $U_{s,av} = U_i / (K/2p) = 477.4/(102/4) = 18.7$ V < 20 V – acceptable
- Maximum voltage between two segments at no-load: $\hat{U}_s = \hat{U}_{i,c} = 2 \cdot N_c \cdot v_a \cdot l \cdot B_{\delta,m} = 2 \cdot 2 \cdot 20.9 \cdot 0.355 \cdot 0.9 = 26.7$ V < 35 V – acceptable
- Maximum voltage between two segments at rated current: Increased field when compared with $B_{\delta,m}$ according to Fig. 10.19b about 25%: $\hat{U}_s = \hat{U}_{i,c} = 1.25 \cdot 26.7 = 33.4$ V < 35 V – acceptable

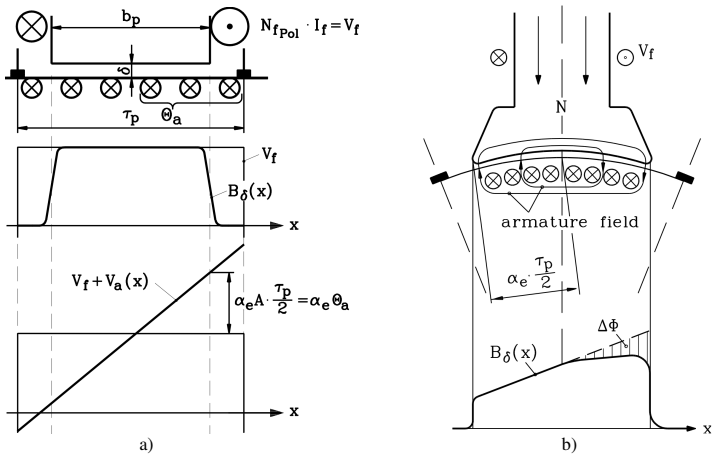

Fig. 10.19: Field distribution at **current carrying armature** of a **not compensated** dc machine:

a) At no-load, the air gap field under one pole is almost constant, because of the constant air gap width δ and the constant exciting ampere-turns V_f. The armature current adds the ampere-turns V_a (armature reaction) to the m.m.f. of the field V_f.

b) The main field is distorted by the armature quadrature-axis field. The increase of the field (right part) is smaller than the decrease (left part), because of the saturation of the iron, resulting in a flux loss $\Delta\Phi$.

Result:

*The **armature reaction** at load causes*

- *a flux loss and hence a reduction of the generated torque and*
- *an increase of the maximum occurring voltage between two segments due to the field distortion.*

d) Compensating Winding:

Machines with large power above about 200 kW...300 kW are designed with **compensating windings**. This winding is arranged in additional slots in the pole shoes of the stator main poles. The compensating winding carries also the armature current, as it is connected in series to plus and minus brushes. The compensating coils are wound to obtain current flow into

opposite direction than the armature current in the rotor slots. Thereby, the compensating winding causes a field in the air gap that is opposite to the rotor air gap field. The number of turns of the compensating coils is designed so that the rotor air gap field and the air gap field of the compensating coils cancel each other. Then, the magnetic field in the air gap does not change between no-load and load, and the performance of the machine is not restricted under load. However, additional copper losses and manufacturing costs of the compensating winding have to be accepted. Slot pitch of rotor and of compensating winding must be designed differently, otherwise a cogging torque would be generated, because the field lines prefer a position where the teeth of stator compensating slots and rotor slots are aligned (**"magnetic cogging torque"**).

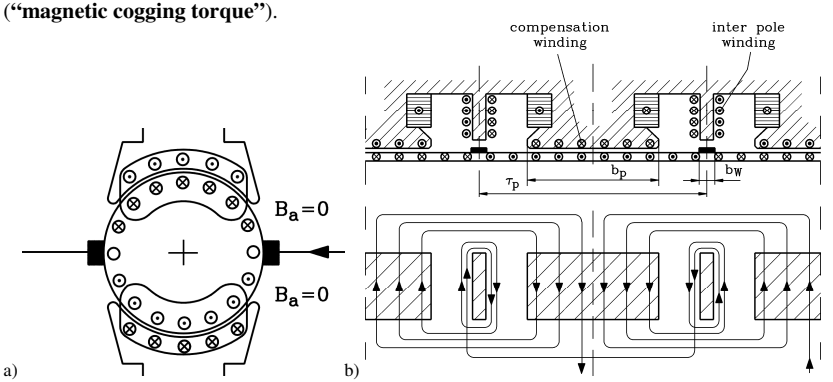

Fig. 10.20: Compensating winding: a) The ampere-turns of armature and compensating winding cancel each other, so that the air gap field does not depend on the armature current, b) Connection of commutating and compensating winding in series

10.5 Commutation of the Armature Current, Basic Function of Commutating Poles

a) Reactance Voltage of Commutation and Sparking During Commutation of Armature Current:

The change of polarity of the armature current from "plus" to "minus" under the brush contact causes some problems. The current per coil i_c changes from a constant positive value $I_a/(2a)$ to the negative value $-I_a/(2a)$, as soon as the brush shorts the two coil terminals of the commutating coil, which are the two neighbouring commutator segments of that coil (Fig. 10.21). At this time, both coil sides are in the neutral zone, so no voltage is induced into the coil by the main field.

Due to the stray flux of slot and winding overhang, each armature coil has an inductance L_c. Therefore, as a result of the current change, a self-induced voltage is generated in the coil u_R, called **"reactance voltage of commutation"**.

$$u_R = L_c \frac{di_c}{dt} \approx L_c \frac{I_a}{a T_{com}} = k_R n I_a \quad , \quad (T_{com} \sim 1/n)$$

$$\boxed{u_R = k_R \cdot n \cdot I_a} \qquad (10.34)$$

The reactance voltage of commutation is estimated by the average **rate of change of the current,** assuming "linear commutation" (Fig. 10.21b):

$$\Delta i_c / \Delta t = 2(I_a/(2a))/T_{com} \qquad (10.35)$$

The **time of commutation** T_{com} is determined by the width of the brush b_b in circumferential direction and the commutator circumferential speed v_C:

$$T_{com} = b_b / v_C \qquad v_C \sim n \qquad \Rightarrow \qquad T_{com} \sim 1/n \qquad (10.36)$$

Result:
The reactance voltage of commutation increases
- *with the load of the machine, hence, proportional with I_a,*
- *with the speed n,*
- *with the magnitude of the armature leakage field, hence with L_C*

Large machines and high-speed machines have a large reactance voltage of commutation.

The first commutator segment of the shorted armature coil separates from the brush at the trailing brush edge. The reactance voltage of commutation as a self-induced voltage delays the current change according to *LENZ*'s law. Therefore, generally, the coil current has not reached its final value $-I_a/(2a)$ – when the trailing brush edge separates from the commutator segment. A current difference Δi_c remains. The rapid change by the value Δi_c to the final value $-I_a/(2a)$ means a high self-induced voltage peak, which ignites sparks between brush and separating segment. This **"sparking"** at the trailing edge of the brush strongly erodes the brush, and the brushes have to be replaced after short time of operation.

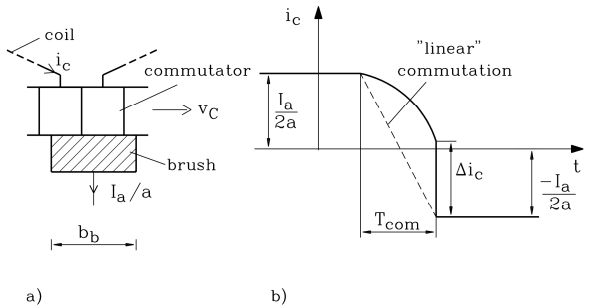

Fig. 10.21: Commutation of the armature current i_c: a) The brush shorts the commutating coil.
b) The coil current changes its polarity, it "commutates".

b) Commutating Poles:
Auxiliary poles (**commutating poles, inter-poles**) are applied in the main pole gaps to avoid the "sparking". These commutating poles are equipped with exciting coils with number of turns per pole $N_{W,pole}$. These coils are connected in series with the armature, so I_a flows there (Fig. 10.20b). The commutating poles excite a magnetic field in the air gap, the **commutating field $B_{\delta W}$**, which is of opposite polarity with respect to the armature quadrature-axis air gap field. Therefore, the armature and the commutating pole flux linkage are oriented opposite in Fig. 10.22. The calculation of the resulting air gap field in the quadrature axis is done by use of *AMPERE*'s law for a closed loop *C*, that represents a field line of the resulting field. It

contains the positive and negative exciting ampere-turns of the main poles, so they have no effect.

$$\oint_C \vec{H} \cdot d\vec{s} = 2\Theta_W - 2\Theta_a + \Theta_f - \Theta_f = 2(\Theta_W - \Theta_a)$$

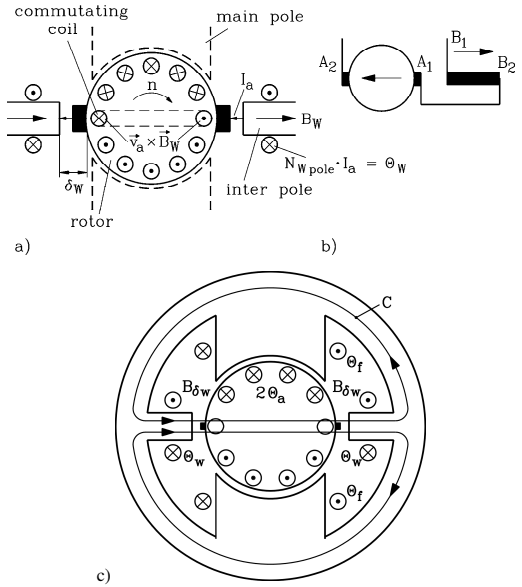

Fig. 10.22: Operating principle of the commutating poles (inter-poles):
a) The commutating poles induce a rotational voltage in the commutating armature coil (compole voltage) of opposite sign than the reactance voltage of commutation, thereby cancelling the latter.
b) The commutating poles carry armature current and are series connected, so that armature and commutating field have opposite sign in the air gap.
c) The ampere-turns Θ_W of the commutating poles must be larger than the armature ampere-turns Θ_a to generate a positive commutating field $B_{\delta W}$ in the air gap.

As the commutating poles are designed for non-saturated iron via a big air gap δ_W, H_{Fe} is almost zero.

$$\oint_C \vec{H} \cdot d\vec{s} = 2H_{Fe,W}\Delta_{Fe,W} + 2H_{\delta,W}\delta_W = 2H_{\delta,W}\delta_W = 2(\Theta_W - \Theta_a) \quad \Rightarrow$$

$$B_{\delta W} = \mu_0 \frac{\Theta_W - \Theta_a}{\delta_W} = \mu_0 \frac{N_{W,pole}I_a - N_{a,pole}I_a}{\delta_W} \sim I_a \qquad (10.37)$$

Result:
The ampere-turns of the commutating poles $N_{W,pole}I_a$ must be chosen slightly larger than those of the armature $N_{a,pole}I_a = z/(8ap)\cdot I_a$, to obtain a positive commutating field in the air gap under the commutating pole δ_W.

The commutating field induces via induction of motion a **compole voltage** u_W of opposite sign with respect to the reactance voltage of commutation, thereby cancelling the influence of u_R.

$$u_W = 2N_c \int_0^l (\vec{v}_a \times \vec{B}_{\delta W}) \cdot d\vec{s} = 2N_c \cdot v_a \cdot l \cdot B_{\delta W} = k_W \cdot n \cdot I_a$$

$$\boxed{u_W = k_W \cdot n \cdot I_a} \qquad (v_a \sim n,\ B_{\delta W} \sim I_a) \qquad (10.38)$$

In order to cancel the influence of u_R, it must be:

$$u_R - u_W = 0 \qquad (10.39)$$

As both u_R and u_W depend on n and I_a, the condition (10.39) is met for EVERY working point of the dc machine, if $k_W = k_R$ is assured by proper design of δ_W and of the ratio $N_{W,pole}/N_{a,pole}$.

$$u_R - u_W = 0 \quad \Rightarrow \quad (k_R - k_W) \cdot n \cdot I_a = 0 \quad \Rightarrow \quad k_R = k_W \qquad (10.40)$$

As the reactance voltage of commutation can only roughly be determined in advance by calculation, it must be verified in the manufacturer's test bay that the brushes do not spark. If necessary, the air gap of the commutating poles must be adjusted by supplementary iron sheets. Condition (10.39) can never be met exactly. Hence, some residual voltage remains during commutating. If the compole voltage is smaller than the reactance voltage of commutation, it is called **under-commutation**, and in the opposite case **over-commutation**. In the case of high overload or overspeed, this residual voltage is sufficiently big, and the machine sparks. Therefore, the calculated reactance voltage of commutation is limited to values taken from experience, which is 10 V for continuous operation and 20 V for intermittent, short-term operation at overload.

10.6 Circuits of DC Generators and Motors

a) Separately Excited DC Generator:
If the machine is driven with constant speed n and the field supplied by an **external**, separate constant dc voltage source (Fig. 10.23a), the main field induces a voltage in the armature that can be measured as no-load voltage U_0 at open armature terminals as function of the exciting current I_f (**no-load characteristic**, Fig. 10.23b). The exciting current is varied via the field regulating resistance R_f.

$$U_0 = k_1 \cdot n \cdot \Phi(I_f) \qquad (10.41)$$

At **load**, the pole flux of a non-compensated machine decreases by the value $\Delta\Phi$. Therefore, the induced voltage is smaller than at no-load (**internal characteristic**, dashed line in Fig. 10.23b).

$$U_i = k_1 \cdot n \cdot \Phi(I_f, I_a) \ < \ U_0 \qquad (10.42)$$

According to the equivalent circuit of Fig. 10.18, considering the voltage drop at the brushes U_b ($U_b \approx 2$ V) and the fact that R_a is the sum of the resistances of the armature, the commutating and the compensating winding resistance, we get:

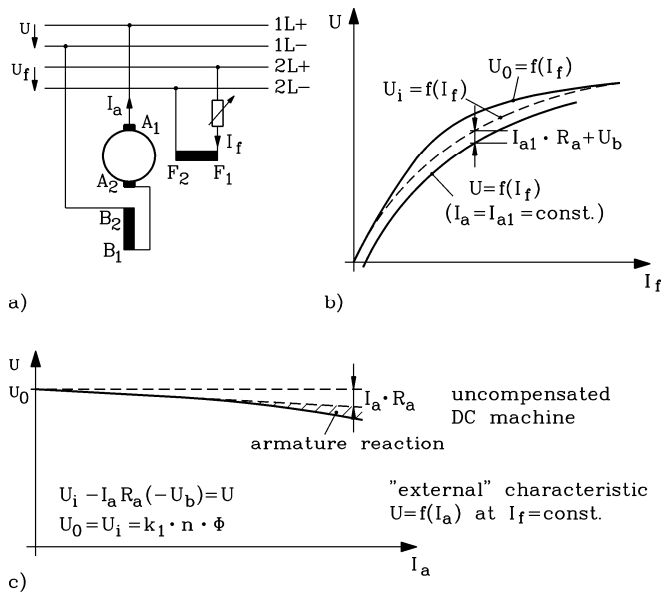

Fig. 10.23: Separately excited dc generator: a) Armature and field circuit, b) no-load characteristic $U_0(I_f)$, internal characteristic $U_i(I_f)$ and load characteristic $U(I_f)$, c) external characteristic $U(I_a)$.

Generator operation: $\boxed{U = U_i - I_a R_a - U_b}$ (10.43a)

Motor operation: $\boxed{U = U_i + I_a R_a + U_b}$ (10.43b)

The function of U – depending on I_f at constant I_a – is called **load characteristic** (Fig. 10.23b); at $I_a = 0$ it is called **no-load characteristic.** Voltage U as a function of I_a at constant I_f it is called **external characteristic** (Fig. 10.23c).

In the case of a compensated machine and at neglected voltage drop at the brushes, the external characteristic is a straight line with a slightly negative slope, caused by the relatively small voltage drop at the resistance R_a. At $I_a = 0$, the no-load voltage U_0 is obtained.

Result:
The separately excited generator produces a voltage U that is almost independent of the load I_a. The voltage U depends on the speed n and the exciting current I_f. Due to the saturation of the main field, U increases non-linear with an increasing exciting current I_f.

In the case of an uncompensated generator, the voltage decreases stronger at load, due to the flux loss $\Delta\Phi$ caused by armature reaction (hatched area in Fig. 10.23c).

Note:
The lettering of the terminals of the dc machine in Figures 10.23 – 10.29 is standardised. The same designations can be found in the terminal boxes of "real" machines.

b) Shunt-Wound Generator:
If the excitation winding is connected in parallel as a **shunt circuit** to the armature winding according to Fig. 10.24a, the driven machine can operate as stand-alone generator which supplies voltage without any external voltage source. The remanence flux Φ_R of the iron stator main poles induces a small **"remanence voltage"** U_R in the rotating armature winding:

$$U_R = k_1 \cdot n \cdot \Phi_R \quad , \qquad (10.44)$$

U_R causes flow of a small field current in the shunted exciting winding:

$$I_f = U_R/(R_a + R_f + R_v) \qquad (10.45)$$

I_f in turn excites a small main flux $\Phi(I_f)$ that increases the remanence flux, so that the induced voltage increases. This again increase the exciting current, so the voltage "builds up" via **self excitation**, until induced voltage and voltage drop at the resistance are balanced. Thereby, the magnetic operating point *A* at no-load is reached (Fig. 10.24b); the machine can supply a load resistance with the armature current I_a. In 1866, the self excitation effect was first published by ***Werner von SIEMENS*** as **"dynamo-electric principle"**.

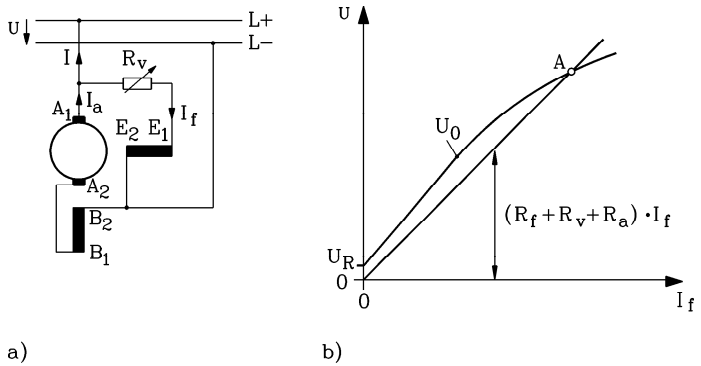

Fig. 10.24: Shunt-wound generator: a) winding circuit, b) no-load operating point *A* due to self excitation $U_0(I_f)$

As the armature voltage decreases at load as a result of the voltage drop at the armature resistance, the exciting current that is driven by the armature voltage also decreases and so does the flux, so that the armature voltage decreases **stronger** at load current than in the case of a separately excited generator, where the exciting voltage is constant.

Significance of the **self excitation**:
Electrical engineering was just evolving 150 years ago. It received an important stimulus by the self-excitation effect. The many early insulated grids could be supplied without use of any permanent magnet generator or battery, which both were not much developed at that time.

Suicide Control:
If the terminals of the exciting circuit are interchanged, the flux excited by the exciting current has opposite polarity with respect to the remanence flux. Hence, it weakens the latter, and the process of self excitation is not started ("suicide"). Where is the "suicide" working point obtained at continuous operation in Fig. 10.24b?

c) Series Wound Generator:

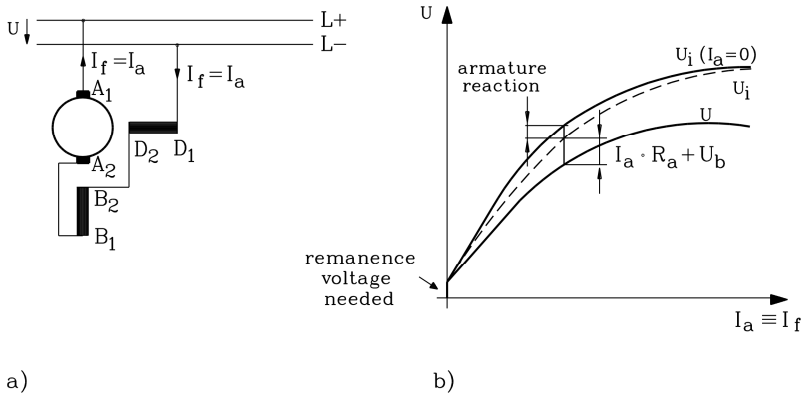

Fig. 10.25: Series wound generator: a) winding circuit; b) The external characteristic is identical to the characteristic at load, because exciting and armature current are identical.

If armature and exciting circuits are connected in series, armature and exciting current are identical:

$$I_a = I_f \qquad (10.46)$$

The remanence voltage itself supplies the "initial voltage" of the machine that is driven at constant speed *n*. At load (= current flow I_a), the main field increases, because the load current equals the exciting current. Therefore, the induced and the terminal voltage *U* increase. At increasing load I_a, the voltage drop at the armature resistance I_aR_a increases linearly, but the induced voltage U_i increases less than linearly. Therefore, the terminal voltage *U* decreases again, despite increasing current I_a. If the voltage drop at the armature equals the induced voltage (**"short-circuit point"**), the terminal voltage becomes zero. This type of generator has only technical relevance as series wound motor allowing for regenerative braking in traction applications (electric train, electric car).

Remark:
In the case of uncompensated machines, the flux loss due to armature reaction must be considered ($U_i < U_0$) (Fig. 10.25b).

d) Shunt-Wound and Separately Excited Motor:
The shunt-wound generator becomes a shunt-wound motor at reversal of the direction of the power flow:
- Reversal of the armature current direction at same armature voltage polarity **or**
- reversal of the voltage polarity at the same current polarity.

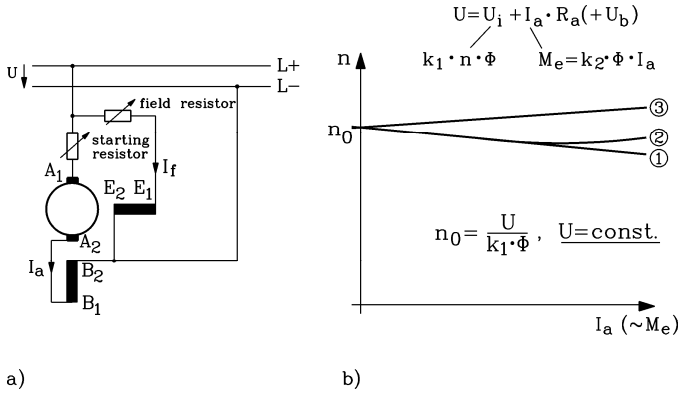

Fig. 10.26: Shunt-wound motor: a) winding circuit, b) motor characteristic *n(M)*: 1: compensated machine, 2: not compensated machine, 3: compensated machine with strong over-commutation

As the voltage grid supplies a constant dc voltage U, the exciting current I_f taken from the grid is also constant. Therefore, the operating characteristic of the **separately excited motor**, where the exciting current is taken from a separate, also constant voltage source, equals that of the **shunt-wound motor**.

At no-load, the motor shaft is not coupled, and the rotor has only to overcome its own small loss torque M_d (friction, rotor iron and armature eddy-current losses). Therefore, $M_e = M_d$ is very small, and the armature current $I_a = M_e/(k_2\Phi)$ is almost zero. Hence, it is $U \cong U_i$. The **no-load speed** n_0 is reached:

$$n_0 = \frac{U}{k_1\Phi(I_f)} \tag{10.47}$$

At load torque M_s at the shaft, the machine generates an electromagnetic torque $M_e = M_s + M_d$ and consumes the armature current $I_a = M_e/(k_2\Phi)$. The consumer reference frame is used: $I_a > 0$ at consumed current = positive current flows **into** the machine.

$$U_i = U - I_a R_a(-U_b) \quad \Rightarrow \quad n = \frac{U_i}{k_1\Phi} = \frac{U - I_a R_a}{k_1\Phi} \tag{10.48}$$

$$\boxed{n = n_0 - \frac{R_a \cdot M_e}{k_1 k_2 \Phi^2} = n_0 - \frac{R_a \cdot M_e}{2\pi k_2^2 \Phi^2}} \tag{10.49}$$

The increasing armature voltage drop reduces the induced voltage with increasing load torque. Therefore, the speed **decreases** due to the decreasing induced voltage.

Result:
Separately excited and shunt-wound motor have a decreasing speed-torque-characteristic with a flat slope, determined by the small armature voltage drop (Fig. 10.26b, Graph 1).

As a first approximation, separately excited and shunt circuit motor have almost constant speed independently of the load (**"stiff *n(M)*-characteristic" – "shunt characteristic"**).

Tendency of instability of a not compensated motor:
In the case of a not compensated machine, with increasing load, the main flux Φ decreases to $\Phi' = \Phi - \Delta\Phi$ due to increased saturation as a result of armature reaction.

$$n = \frac{U}{k_1 \cdot (\Phi - \Delta\Phi(I_a))} - \frac{R_a \cdot I_a}{k_1 \cdot (\Phi - \Delta\Phi(I_a))} \tag{10.50}$$

Due to the flux decrease with increasing load, the speed decreases less than in the case of constant flux. In the case of large I_a and hence large flux loss $\Delta\Phi$, the speed even increases again, because the first term in (10.50) increases stronger than the second term decreases (Fig. 10.26b, Graph 2). At uncontrolled operation, this **increase of speed at increasing load** torque M_s is **not stable** (Section 10.8). The machine **"runs away"**, it accelerates instantaneously to high speed up to self-destruction.

Instability of an over-commutating motor:

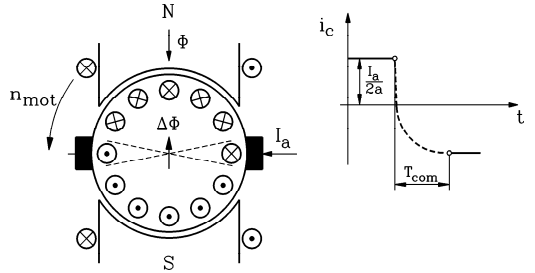

Fig. 10.27: Over-commutation:
a) The commutating coil has, due to too fast commutation, already reversed coil current and coil flux linkage, hence, it excites a coil flux $\Delta\Phi$ that weakens the main flux Φ.
b) The current commutation is too fast, due to a too large commutating field.

In the case of **over-commutation**, the commutating field is too strong. Therefore, the current commutation is faster than linear commutation. Already shortly after the coil is short-circuited via the brushes, the coil current has already reversed polarity (Fig. 10.27b). Therefore, the commutating coil of Fig. 10.27a has already reversed flux linkage and excites a flux linkage $\Delta\Phi \sim I_a$, which counteracts and thereby weakens the main flux Φ. This effect happens already at small armature current. If the flux weakening is **stronger** than the voltage drop $R_a I_a$, the speed-torque characteristic is a straight line with positive slope.

Result:
*A dc shunt-wound motor with strong over-commutation may become **unstable** already at small load.*

Starting resistance in the armature circuit:
The **starting resistance** shown in the armature circuit of Fig. 10.26a serves to limit the armature current during starting the motor. At zero speed, the induced voltage is zero, and the voltage drop at the armature equals the line voltage: $U = I_a R_a$. As the armature resistance – except for small-power motors – is very small, the armature current at zero speed would be a multiple of the thermal permissible continuous current, and the motor winding would be destroyed by overheating. Accordingly, an additional "starting resistance" is used series connected to limit the armature current to rated current:

$$(R_{starter} + R_a) \cdot I_N = U \quad \Rightarrow \quad R_{starter} = \frac{U}{I_N} - R_a \tag{10.51}$$

After start-up, the induced voltage limits the current; the starter resistance $R_{starter}$ is shorted to avoid its copper losses.

Example 10.6-1:
DC motor: U_N = 430 V, P_N = 200 kW, η = 92% (without excitation losses), R_a = 37.9 mΩ

- Rated current: $I_N = P_N / (\eta \cdot U_N) = \underline{\underline{506}}$ A
- Start-up without starting resistor: $I_a = U_N / R_a = 430 / 0.037 = \underline{\underline{11350}}\ A = \underline{\underline{22.4}}$ times rated current
- Necessary starting resistance: $R_{starter} = \frac{U_N}{I_N} - R_a = \frac{430}{506} - 0.0379 = \underline{\underline{0.8\Omega}}$

d) Series-Wound Motor:

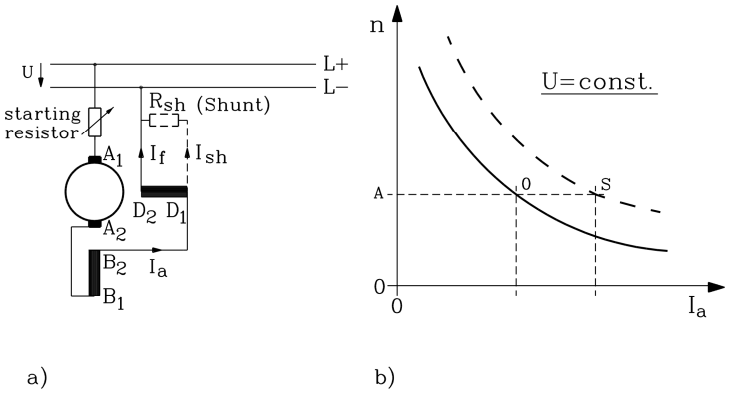

Fig. 10.28: Series-wound motor: a) winding circuit, b) motor characteristic *n(M)* without (full line) and with external shunt resistance R_{sh} (dashed line)

As excitation and armature current are identical, the generated electromagnetic torque is:

$$M_e = k_2 \Phi(I_a) I_a \tag{10.52}$$

If the saturation is assumed to be constant as a rough approximation and hence, the flux is proportional to the armature current ($\Phi = L' \cdot I_a$), the torque increases **with the square** of the armature current:

$$M_e = k_2 \cdot L' I_a^2 \tag{10.53}$$

In the case of small armature currents and hence small flux, this is exactly true, because the saturation of the iron occurs at larger flux values. For neglected brush voltage drop $U_b \approx 0$, we get from (10.43):

$$n = \frac{U - I_a R_a}{2\pi k_2 \Phi} = \frac{1}{2\pi k_2 L'} \left(\frac{U}{I_a} - R_a \right) = \frac{U}{2\pi \sqrt{k_2 L'}} \cdot \frac{1}{\sqrt{M_e}} - \frac{R_a}{2\pi k_2 L'} \tag{10.54}$$

Result:
The speed of a series-wound motor decreases nearly hyperbolically with the load torque $M_e \approx M_s$ down to zero speed.

A series-wound motor **must not be operated without any load**, because then it accelerates up to theoretically infinite speed as the load disappears ($M_s = 0$) (**"run-away"**) and is destroyed. The strong decrease of speed with increasing load is called **"soft characteristic"** (**"series-wound characteristic"**).
The series-wound motor is well suited for traction (electric train, electric car). In the case of small motor speed ("start-up"), the torque is high and can accelerate the vehicle. A certain load is always given by the contact between wheel and track (rolling resistance) and by the aerodynamic resistance. Therefore, run-away cannot happen under usual operation conditions. However, the drive must be protected by an overspeed limiter for the case of wheel-spinning (**"sliding"**) due to loss of the contact between wheel and road (e.g. in the case of a wet track).

Speed Control by Flux Weakening with a Shunt Resistance:
The field exciting current can be reduced by means of a **shunt resistance R_{sh}** in parallel to the field winding. Hence, at constant motor terminal voltage and load, the speed can be controlled by flux weakening. The field current I_f is by the factor ξ smaller than the armature current I_a. In the same way, the flux decreases; at constant armature current, the speed increases by the factor $1/\xi$.

$$I_f R_f = I_{sh} R_{sh} = (I_a - I_f) R_{sh} \quad \Rightarrow \quad \frac{I_f}{I_a} = \frac{R_{sh}}{R_{sh} + R_f} = \xi \tag{10.55}$$

$$n = \frac{U - I_a R_a}{2\pi k_2 \Phi(I_f)} = \frac{U - I_a R_a}{2\pi k_2 L' I_f} = \frac{U - I_a R_a}{2\pi k_2 L' \xi I_a} = \frac{1}{\xi} \cdot \frac{1}{2\pi k_2 L'} \left(\frac{U}{I_a} - R_a \right) \tag{10.56}$$

f) Compound-Wound Machines:
If both series and shunt winding are used, an additional degree of freedom is obtained. The series winding – characterised by a small number of turns with large cross sectional area of conductors to carry the armature current – and the shunt winding – characterised by a high number of turns with small cross sectional area of conductors to carry the generally small exciting current – can be adjusted e.g. at *generator operation*, so that the motor terminal voltage is the same at no-load and at rated current (**"normal compounding"**). In the load

range in-between, a certain over-voltage exists. At *motor operation*, the stiff shunt characteristic can become slightly softer by a small series winding (**auxiliary series winding**) that excites a flux of about 10 % of the shunt circuit flux. Furthermore, the flux decrease $\Delta\Phi$ due to armature reaction can be partly compensated by the auxiliary flux excited by the series winding (Fig. 10.29).

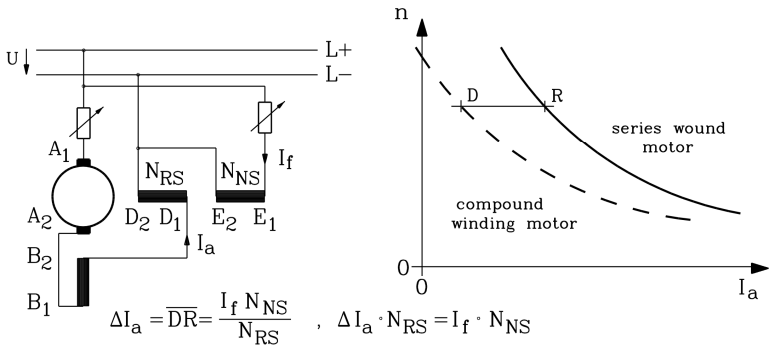

Fig. 10.29: Compound winding motor: a) winding circuit, b) motor characteristic *n(M)*

10.7 Variable Speed DC Drives

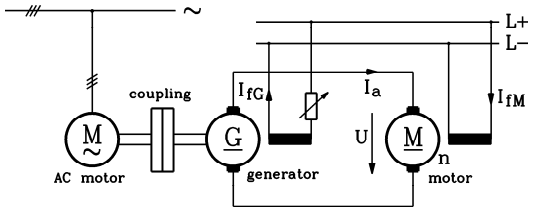

Fig. 10.30: A dc motor can be operated at variable speed by means of a *WARD-LEONARD*-converter.

In most industrial applications, DC drives operated as **variable speed drives** are mostly connected as **separately excited machines**. According to (10.57), the speed can be controlled by **three parameters**:

A) control of the armature voltage U,
B) flux weakening of Φ (flux increase is not used, due to increased saturation)
C) series connection of a variable resistance in the armature circuit.

Variable series resistance C) is nowadays only rarely used, because of the increased copper losses. However, it was used in electric streetcars, operated from a dc grid, e.g. at 750 V, for speed variation before the advent of power electronics.

$$n = \frac{U_i}{k_1\Phi} = \frac{U - I_a R_a}{z\frac{p}{a}\Phi} \qquad (10.57)$$

a) WARD-LEONARD-converter:
Alternative A) "voltage control":
At ac line operation, voltage control can be performed by rotating machines using the classical ***WARD-LEONARD*-converter** (Fig. 10.30). A line-operated ac induction motor drives a separately excited dc generator G at almost constant speed n_{IM}. Its exciting current I_{fG} is supplied by a further small rotary converter, e.g. an ac induction motor and self-excited shunt circuit generator or a battery. This generator G generates a variable armature voltage U that feeds a dc motor, which is separately excited by I_{fM}. Thus the speed of the dc motor n can be directly controlled via the variable voltage U of the generator G.

Alternative B) "flux weakening":
The exciting current I_{fM} of the motor allows weakening of the flux to make further increase of the speed possible, when the generator voltage U has reached its maximum value.

Today, the *WARD-LEONARD*-rotary converter is only rarely used, because
(i) **three times** the full machine power is installed (expensive!),
(ii) **three times** the full losses occur (e.g., efficiency per machine 90 % results in 73 % overall efficiency!),
(iii) it is a **dynamically low quality** drive. The field of the controlling generator cannot be increased rapidly to increase the motor speed quickly. The inductance L_f of the field winding of generator G is very large, because of the high number of turns in the field winding coils, so the electric field time constant $T_f = L_f / R_f$ is large. Therefore, the voltage change happens only slowly, within some seconds, so dynamic speed control of the motor is not possible.
(iv) The reactive power is determined by the $\cos\varphi$ of the induction machine, which has a value of about 0.85.

Four-Quadrant Operation with use of the WARD-LEONARD Converter:
The **control generator G** in Fig. 10.30 supplies negative voltage if the terminal connections are exchanged, so that the motor speed can be reversed. Therefore, two quadrant operation is possible at motor operation, which are – in the consumer reference frame – the **first quadrant** ($I_a > 0$, $n > 0$) and the **third quadrant** ($I_a < 0$, $n < 0$) in Fig. 10.31a. Furthermore, the power flow can be reversed. If the dc motor is externally driven, it becomes a generator. At constant speed, the polarity of the armature current reverses, if the induced voltage of the dc motor is larger than the sum of the induced voltage of the generator G and the voltage drop at the armature resistances of both dc machines. The control generator G becomes a motor and drives the induction machine supersynchronously, so that the latter feeds active power back into the grid as generator. This is possible for both directions of rotation of the dc motor, so that also the **second** and the **fourth quadrant** ($I_a < 0$, $n > 0$); ($I_a > 0$, $n < 0$) of the set of characteristic curves of Fig. 10.31a can be covered (**four-quadrant operation**).

b) Operating Limits of Separately Excited DC Machines at Four-quadrant Operation:
A) **"Control by armature voltage": U_a/U_{aN} varied (Fig. 10.31b)**
The set of speed-torque curves is limited by the thermally maximum permissible armature current and the constant flux at maximum armature voltage U. For the maximum values of the operational parameters U_a, I_a, Φ, M and P as a function of n, it is:

Armature voltage control region: $0 \le n \le n_N$:

$U_a \sim n$, $I_a = I_N$ = const., $\Phi = \Phi_N$ = const., $M = M_N \sim I_a\Phi$ = const., $P = U_aI_a = 2\pi nM \sim n$

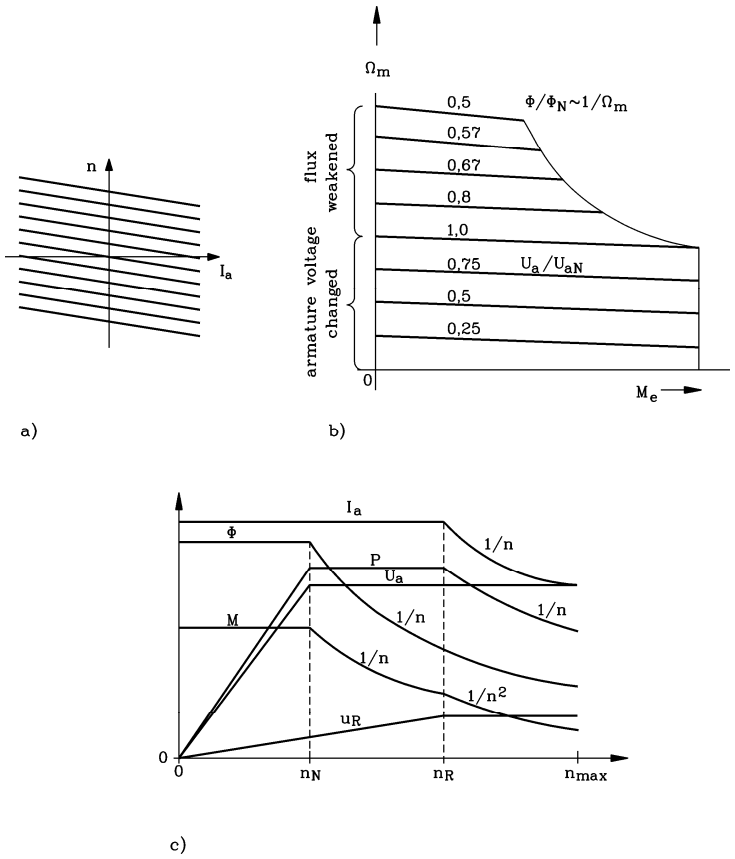

Fig. 10.31: Set of characteristic curves of a separately excited (compensated) dc motor at supply with variable voltage U_a and variable flux Φ
a) torque-speed characteristic at variable armature voltage, four-quadrant operation,
b) torque-speed characteristic at armature voltage control and flux weakening (one quadrant operation)
c) maximum values of armature voltage, armature current, torque, flux, power and reactance voltage of commutation.

B) **"Flux weakening region" (constant power region): Φ/Φ_N varied (Fig. 10.31b)**

Higher motor speed above $n_0 = U_{max}/(k_1 \cdot \Phi_N)$ can be obtained by flux weakening. At constant, maximum armature current I_N, the maximum torque decreases proportionally with decreasing flux. The slope of the *n(M)*-characteristic is proportional to $1/\Phi^2$ according to (10.49). Therefore, at **flux weakening**, the slopes of the *n(M)*-curves are steeper than at full flux at armature voltage control. The maximum values of the operational parameters U_a, I_a, Φ, M and P as a function of n are (Fig. 10.31c):

Flux weakening region: $n_N \le n \le n_{max}$:

$U_a = U_N$ = const., $I_a = I_N$ = const, $\Phi \sim 1/n$, $M \sim I_a\Phi \sim 1/n$, $P = U_NI_a = 2\pi nM = P_N$ = const.

Result:

At armature voltage control, the maximum power that can be converted, increases linearly with the speed. It is constant in the speed range of field weakening.

C) **Commutation Limit (black band limit): $n_R \le n \le n_{max}$:**

At high motor speed in the flux weakening range, the reactance voltage of commutation may become so high that the permissible limit of 10 V is exceeded above a certain motor speed n_R. This will lead to heavy sparking. Therefore, the armature current must be reduced above this speed to maintain the reactance voltage u_R constant (Fig. 10.31c).

The flux weakening region is reduced to $n_N \le n \le n_R$ and the **limit of commutation** is determined by: $n_R \le n \le n_{max}$:
$U_a = U_N$ = const., $u_R = k_R\, nI_a$ = 10 V, $I_a \sim 1/n$, $\Phi \sim 1/n$, $M \sim I_a\Phi \sim 1/n^2$,
$P = U_NI_a = 2\pi nM = 1/n$.

c) Controlled Bridge Circuit Rectifier for DC Machine Supply:

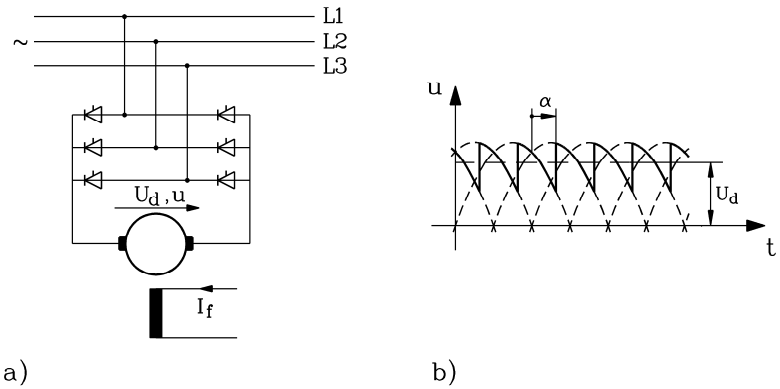

Fig. 10.32: Controlled ac bridge rectifier B6C for supply of a variable speed separately excited dc machine, a) bridge circuit for one current direction, b) rectified voltage at the armature terminals

The variable dc voltage U can be generated from the ac grid by rectification via a thyristor bridge (**controlled rectifier**). Likewise, the variable field current I_f is generated via a controlled rectifier. **Today**, this is the **state-of-the-art solution**, because it is dynamic as a change of the rectified voltage is possible within several ms, and the losses are low. The efficiency of rectification is higher than 97%.

Operating principle of controlled rectification:

Fig. 10.32a shows a line-operated, controlled bridge circuit rectifier in **six-pulse** connection, which is supplied by the line-to-line voltage U_{grid} (r.m.s.-value). Each of the six thyristors conducts one third of the period time of the line voltage, in which always two thyristors – one at plus and one at minus of the armature – are conducting at the same time. If the firing angle α is set to zero, the thyristors are line-commutated at the natural commutation point. The

connection acts as a diode bridge rectifier, and the average value of the rectified voltage with its six voltage ripples per grid period has its maximum value $U_{d,m}$. Here, the influence of the finite time of commutation of the thyristors is neglected.

$$U_{d,m} = \frac{3}{\pi}\sqrt{2}U_{grid} \tag{10.58}$$

If the **firing angle** α is increased, the average voltage U_d decreases according to (Fig. 10.32b):

$$U_d = U_{d,m} \cdot \cos\alpha \tag{10.59}$$

At $\alpha = 90°$, the average value of the rectified voltage is zero, at $\alpha > 90°$, the rectified voltage is negative: $U_d < 0$.

Result:
A controlled bridge rectifier allows variation of the armature voltage U from $-U_{d,m}$ (at $\alpha = 180°$) up to $+U_{d,m}$ (at $\alpha = 0°$).

One disadvantage are the voltage harmonics of six, twelve, etc. times line frequency contained in the rectified voltage, due to the voltage ripple. The **armature inductance L_a is very small**, because the armature field and the commutation field almost cancel each other (see Section 10.5). Therefore, they only slightly smooth the armature current. Accordingly, the armature current and the armature field also contain these harmonics, leading to increased losses and noises (e.g. **magnetically generated 300 Hz-sound**, because it is 6·50 = 300 Hz).

Four-quadrant operation with controlled rectification:
The connection shown in Fig. 10.32a allows operation in the first and the fourth quadrant of the n-I_a-plane, because the thyristors allow only current flow in positive direction (valve effect). Another controlled bridge rectifier using antiparallel thyristors is needed to allow for current flow into negative direction (**"reversible converter"**, **"double-way converter"**). Thereby, operation in the second and third quadrant is possible.

The **exciting current** I_f is also supplied by a controlled rectifier bridge. The large inductance of the field winding L_f smoothes the field current very well, so that I_f is almost an ideal dc current. However, some residual pulsation of the main field remains, which induces an additional voltage into commutating armature coils (**"transformer spark voltage"**). Especially in the case of small machines with a high number of turns of the armature winding, this additional voltage is large enough to cause additional sparking at the brushes.

d) DC Chopper Supplying DC Machines:
In the case of dc chopper operation, a constant dc voltage U is chopped by means of transistor switches. The voltage U may be supplied by an uncontrolled dc rectifier with a smoothing capacitor, or by a battery (Fig. 10.33a).

With modern power transistors, the **pulse frequency** as given by (10.60) is relatively high (at least 1 to 2 kHz)

$$f_P = 1/T \tag{10.60}$$

The chopped voltage is supplied to the dc machine as the armature voltage. The average value U_d of the chopped armature voltage u_a can be **varied** from 0 up to U by the variable ratio of pulse width and pause (Fig. 10.33b). The transistor is turned on during the pulse width time

T_{on} and current flows from the voltage source U to the machine. The free wheeling diode is at zero current.

$$U_d = U\frac{T_{on}}{T} \tag{10.61}$$

The transistor is turned off during the pause, but the current flow must continue, because of the self-induced voltage due to the armature circuit inductance. This is possible via the **free wheeling diode**. Due to the relatively high chopping frequency, the rather small armature inductance can smooth the armature current so that the latter is almost free of harmonics (only small "saw tooth ripples" with chopping frequency, Fig. 10.33b). The chopper of Fig. 10.33a is suitable for one quadrant operation. It can be extended by three additional transistors and free-wheeling diodes to allow for four-quadrant operation.

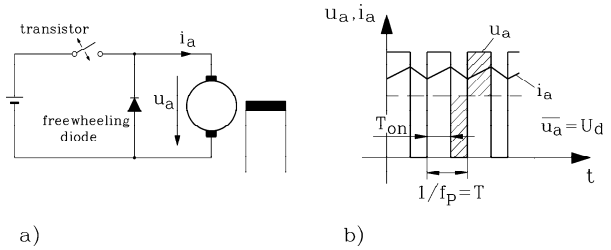

Fig. 10.33: DC chopper: a) principle of operation, b) chopped armature voltage, its average value and armature current

10.8 Efficiency, Stability and Operational Limits of DC Machines

a) Efficiency:
The following losses occur at **no-load** (armature current is zero):
A) **Iron losses in the rotor iron:** The rotor rotates in the dc stator field. Eddy currents with armature frequency $n \cdot p$ are induced in the rotor. Therefore, it must be laminated, to disrupt the eddy-current paths. Furthermore, hysteresis losses occur.
B) **Mechanical** friction losses of bearings, air and brushes, as well as windage losses, if a fan is applied.
C) **Additional no-load losses:** Eddy-currents in rotor winding due to harmonics of the air gap field.
Load-dependent losses occur at **load** due to flow of armature current:
D) **Copper losses** in the armature, commutating and compensating winding or auxiliary series winding,
E) **Resistive losses** in the brushes,
F) **Load dependent additional losses**: Eddy-current losses in the slot conductors in the rotor, because of the ac current flow in the armature winding.
Excitation losses occur both at no-load and at load in the field winding as resistive losses $R_f I_f^2$.

Due to the losses in the commutation and compensating winding and in the commutator-brush-system, the efficiency of dc machines is generally **somewhat smaller** than the efficiency of ac machines of same rated power and size.

b) Stability of Operating Points:
The quasi-static stability of the operating points of a dc machine is determined in the same way as in the case of an induction machine (Section 7.3). This is explained using the example of a separately excited dc motor with flux loss $\Delta\Phi$ due to armature reaction. The condition for stability is (Section 7.3):

$$\frac{dM_e}{d\Omega_m} - \frac{dM_s}{d\Omega_m} < 0 \quad \Rightarrow \quad stable \tag{10.62}$$

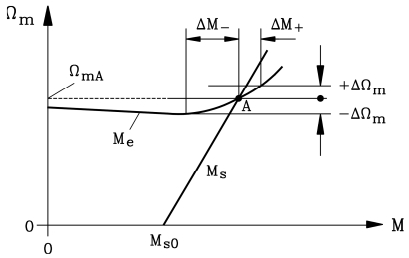

Fig. 10.34: At high load, this non-compensated shunt-wound motor does not operate stable, with the applied load.

In Fig. 10.34, it is assumed that the load torque at the motor shaft increases linearly with speed, starting with a breakaway torque M_{s0} at $n = 0$ ($\Omega_m = 2\pi n$). The point of intersection A with the motor characteristic gives the speed Ω_{mA}, which is in the range, where the motor speed **increases** with increasing load. Both $dM_e/d\Omega_m$ and $dM_s/d\Omega_m$ are positive; their difference is also positive, so that the criteria for stability (10.62) is not met. The drive does not operate stable and speed will increase quickly.

c) Operational Limits:
The size and hence the power that can be installed per dc machine unit (**"unit rating"**) are limited by the commutator:
- centrifugal force limit: Speed limit, otherwise deformation of the commutator, leading to brush bouncing
- commutation limit: Speed limit to keep reactance voltage of commutation $u_R < 10$ V continuously, < 20 V intermitt-ent, otherwise heavy sparking occurs,
- brush current density: Current limit to get $J_b < 12$ A/cm^2 continuously, < 20 A/cm^2 intermittent, otherwise the brushes wear out too fast,
- voltage limit to keep average segment voltage $U_{s,av} < 20$ V, local segment voltage < 35 V, otherwise flashover might occur.

At uncontrolled operation, the **limit of stability** exists additionally, so that the separately excited motor can usually be operated only in the region of negative slope of the $n(M)$-characteristic.

The **largest dc machines** have been designed as steel-mill drives with rated power from 6 MW up to 12 MW at rated motor speed of about 100/min. The power can be further increased only by series coupling of two machines (**"tandem" design**). Due to the limited unit rating, large dc machines are nowadays replaced by inverter-fed synchronous machines (up to 100 MW) and induction machines (up to 30 MW). Furthermore, in the lower power range, the more robust inverter-fed induction motor with field oriented control is preferred, because it requires less maintenance.

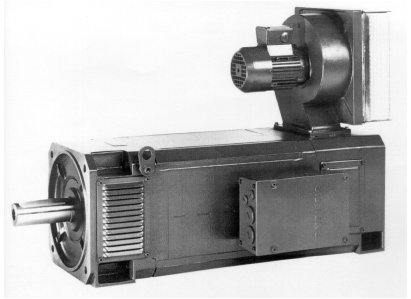

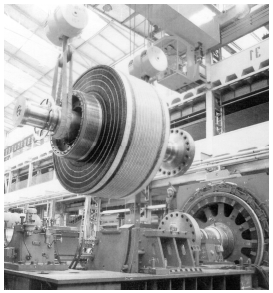

Fig. 10.35: Separately excited dc machines: left: four pole machine with additional external fan, right: 2 x 12 MW-mill drive in "tandem": Mounting of the rotor of the first machine, the second machine behind is already completed.

10.9 Dynamic Equations of DC Machines

The equations for **steady state operation** contain only dc quantities. We note in the consumer reference frame:

$$\begin{aligned} U &= I_a R_a + U_i (+U_b) \\ U_i &= k_2 \Omega_m \Phi \\ \Phi &= \Phi(I_f) \\ M_e &= k_2 \Phi I_a \\ U_f &= I_f R_f \end{aligned} \tag{10.63}$$

In the case of **dynamic operation**, not only motor speed and armature current, but also armature voltage, exciting current and voltage and hence main flux may change with time. Hence, the field excited by the armature current – represented by the **armature self-inductance** L_a – also changes and causes an additional self-induced voltage in the armature circuit. This field is **small**, because the commutating winding counteracts with the armature field, so that only the armature leakage field in the slot and winding overhang remains as effective self-inductance.

The variation of the main flux also causes an additional self-induced voltage in the field circuit, which is represented by the **field self-inductance** L_f. This inductance is **large**, because of the large main flux and the generally high number of turns of the field winding.

A **mutual inductance** M_{af} between armature coils and field coil does not exist, because only the just commutating coil is linked like in a transformer with the main field. All other, series connected armature coils are only induced by the main field via motion induction. If the commutating coil is neglected, only L_a and L_f have to be considered for the dynamic equations.

$$u(t) = i_a(t) \cdot R_a + L_a \cdot \frac{di_a(t)}{dt} + u_i(t) \tag{10.64}$$

$$u_i(t) = k_2 \Omega_m(t) \Phi(t) \tag{10.65}$$

$$\Phi(t) = \Phi(i_f(t)) \tag{10.66}$$

$$M_e(t) = k_2 \Phi(t) i_a(t) \tag{10.67}$$

$$u_f(t) = i_f(t) \cdot R_f + L_f \cdot \frac{di_f(t)}{dt} \tag{10.68}$$

The **dynamic equation of motion** (Chapter 7) adds to this set of equations. Here the loss torque in the machine M_d is neglected for simplification, so that the internal torque M_e is taken as total motor torque.

$$J \cdot \frac{d\Omega_m(t)}{dt} = M_e(t) - M_s(t) \tag{10.69}$$

Thanks to the simple structure of the **dynamic equations**, the dc machine is simple to control. The armature current that controls the torque is itself directly controlled via the armature voltage. The torque influences the motor speed. The current variation occurs very fast: the **armature time constant** $T_a = L_a/R_a$ is as small as a few milliseconds, depending on the size of the machine.

Example 10.10-1:
If, at $\Phi = \text{const.}$, $\Omega_m = \text{const.}$ and beginning at no-load ($U = U_i$), the armature voltage is increased by ΔU, (10.64) gives:

$$U + \Delta U = i_a \cdot R_a + L_a \cdot \frac{di_a}{dt} + U_i \quad \Rightarrow \quad L_a \cdot \frac{di_a}{dt} + i_a \cdot R_a = \Delta U$$

This is a first order linear differential equation with constant coefficients and the following solution:

$$i_a(t) = \frac{\Delta U}{R_a} \cdot (1 - \exp(-t / T_a)) \qquad \text{where} \quad \boxed{T_a = L_a / R_a} \tag{10.70}$$

Result:
The armature current changes with the armature time constant T_a.

The change of torque via the main field is much slower, because the field current I_f that excites the main field changes with the **large field time constant** $T_f = L_f/R_f$ (typically some seconds). Starting at $U_{f0} = I_{f0} R_f$, the current i_f changes with a voltage step ΔU_f:

$$U_{f0} + \Delta U_f = i_f \cdot R_f + L_f \cdot \frac{di_f}{dt} + I_{f0} R_f \qquad \Rightarrow \quad L_f \cdot \frac{di_f}{dt} + i_f \cdot R_f = \Delta U_f$$

This is a first order linear differential equation with constant coefficients and the following solution:

$$i_f(t) = \frac{\Delta U_f}{R_f} \cdot (1 - \exp(-t / T_f)) \qquad \text{where} \quad \boxed{T_f = L_f / R_f} \tag{10.71}$$

Result:
The exciting field current changes with the field time constant T_f. Therefore, dc machines are controlled via the armature circuit, which is much faster. The armature voltage is the control parameter. It is varied by a converter. The field circuit is used for the much slower field weakening.